Journal of Hydrology 652 (2025) 132684

Contents lists available at ScienceDirect

Journal of Hydrology

journal homepage: www.elsevier.com/locate/jhydrol

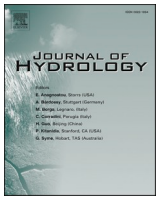

Identifying the influence of hydroclimatic factors on streamflow: A multi-model data-driven approach

Khandaker Iftekharul Islam [a,*], James Matthew Gilbert [a,b]

[a] University of California, Santa Cruz, Institute of Marine Sciences' Fisheries Collaborative Program, 1156 High Street, Santa Cruz, CA 95064, USA
[b] Fisheries Ecology Division, Southwest Fisheries Science Center, National Marine Fisheries Service, National Oceanic and Atmospheric Administration (NOAA), 110 McAllister Way, Santa Cruz, CA 95060, USA

ARTICLE INFO

This manuscript was handled by Emmanouil Anagnostou, Editor-in-Chief

Keywords:
Bayesian model averaging
Ensemble machine learning
Multimodal inferences
Streamflow drivers
Climate change

ABSTRACT

Climate change impacts water supply dynamics in the Upper Rio Grande (URG) watersheds of the US Southwest, where declining snowpack and altered snowmelt patterns have been observed. While temperature and precipitation effects on streamflow often receive the primary focus, other hydroclimate variables may provide more specific insight into runoff processes, especially at regional scales and in mountainous terrain where snowpack is a dominant water storage. The study addresses the gap by examining the mechanisms of generating streamflow through multi-modal inferences, coupling the Bayesian Information Criterion (BIC) and Bayesian Model Averaging (BMA) techniques. We identified significant streamflow predictors, exploring their relative influences over time and space across the URG watersheds. Additionally, the study compared the BIC-BMA-based regression model with Random Forest Regression (RFR), an ensemble Machine Learning (RFML) model, and validated them against unseen data. The study analyzed seasonal and long-term changes in streamflow generation mechanisms and identified emergent variables that influence streamflow. Moreover, monthly time series simulations assessed the overall prediction accuracy of the models. We evaluated the significance of the predictor variables in the proposed model and used the Gini feature importance within RFML to understand better the factors driving the influences. Results revealed that the hydroclimate drivers of streamflow exhibited temporal and spatial variability with significant lag effects. The findings also highlighted the diminishing influence of snow parameters (i.e., snow cover, snow depth, snow albedo) on streamflow while increasing soil moisture influence, particularly in downstream areas moving towards upstream or elevated watersheds. The evolving dynamics of snowmelt-runoff hydrology in this mountainous environment suggest a potential shift in streamflow generation pathways. The study contributes to the broader effort to elucidate the complex interplay between hydroclimate variables and streamflow dynamics, aiding in informed water resource management decisions.

1. Introduction

Climate change is driving impacts on water supply across the Southwest of the United States. In the Upper Rio Grande (URG) Basin, these changes arise through declining snowpack and decreases in projected runoff per unit snowpack volume (Chavarria and Gutzler, 2018; Holmes et al., 2022). In addition, changing climate patterns influence snowpack characteristics like snow accumulation and ablation (Liao and Zhuang, 2017; Taia et al., 2023), affecting the quantity and timing of runoff in the snow-dominated watersheds within the San Juan Mountain range of the URG (Moeser et al., 2021). These watersheds of the URG serve as a critical upstream source for the Rio Grande Basin (RGB), which provides municipal water for over 6 million people and irrigation water for 2 million acres of land (Rio Grande Basin, 2016). Continuing climate change will likely impact regional natural streamflow generation (Lehner et al., 2017; Moeser et al., 2021), requiring a better understanding of regional factors affecting streamflow, particularly those attributed to climate change. Anticipated effects of climate change on hydro-climatic factors in the watersheds may lead to a compounded reduction in runoff where multiple factors contribute to a cumulative decrease (Islam et al., 2023, 2022, 2019), with potential consequences for agriculture, ecosystems, and socio-technical systems in the region.

A changing water supply challenges water managers; models are often used to provide insight into future hydrologic conditions (Islam,

* Corresponding author at: Institute of Marine Sciences, Physical and Biological Sciences Division, University of California, Santa Cruz, USA
E-mail addresses: kiislam@ucsc.edu, iftikhar.islam41@gmail.com (K.I. Islam), james.gilbert@ucsc.edu (J.M. Gilbert).

https://doi.org/10.1016/j.jhydrol.2025.132684
Received 19 August 2024; Received in revised form 1 December 2024; Accepted 5 January 2025
Available online 13 January 2025

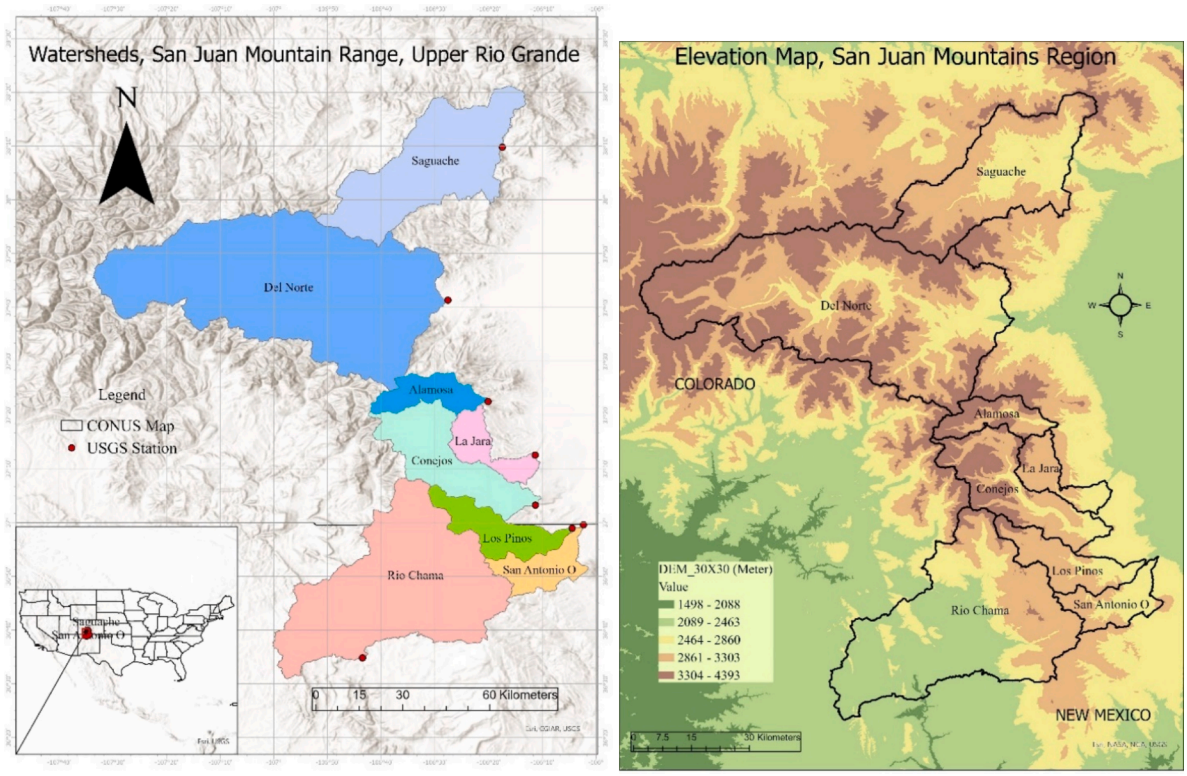

Fig. 1. (A) Study watersheds of the San Juan Mountains, (B) Elevation map.

Table 1
USGS gauging stations, watershed areas, latitude, longitude, and elevation ranges.

San Juan Mountains' Watersheds	USGS Gauging Station	Watershed Area (sq-km)	Watershed within Latitude	Elevation Range (m.a.s.l)	Average Elevation (m)	Total Precip. (mm/year)	Avg. Min Temp (°C)
Saguache	8227000	1340	37°50′–38°20′	2448–4229	3338.5	524.28	2.79
Del Norte	8220000	3396	37°25′–38°00′	2436–4222	3330.5	755.04	1.69
Alamosa	8236000	274	37°20′–37°30′	2624–4036	3330	898.96	1.95
Conejos	8246500	729	37°00′–37°25′	2524–4005	3264.5	972.72	2.56
Los Pinos	8248000	395	36°50′–37°10′	2454–3716	3085	891.6	3.48
Lajara	8238000	266	37°05′–37°25′	2464–3632	3048	738.12	3.65
Rio Chama	8285500	1222	36°30′–37°10′	2159–3886	3022.5	642.6	5.29
San Antonio-Ortiz	8247500	298	36°45′–37°00′	2437–3327	2882	628.32	4.18

Table 2
Time series variables and respective data format and sources.

Variable	Type of data	Unit	Data description	Reference
SWE	Raster-Monthly	kg/m^2	NLDAS-2 Mosaic Land Surface Model	(Mocko, 2012; Rui and Mocko, 2018)
Snow Depth	Raster-Monthly	(m)	NLDAS-2 Mosaic Land Surface Model	(Mocko, 2012; Rui and Mocko, 2018)
Snow Cover	Raster-Monthly	Fraction	NLDAS-2 Mosaic Land Surface Model	(Mocko, 2012; Rui and Mocko, 2018)
Min. Temperature	Raster-Monthly	℃	PRISM Climate Data	("PRISM Climate Group," 2014)
Precipitation	Raster-Monthly	mm	PRISM Climate Data	("PRISM Climate Group," 2014)
Snow Albedo	Raster-Monthly	%	NLDAS-2 Mosaic Land Surface Model	(Mocko, 2012; Rui and Mocko, 2018)
Sublimation	Raster-Monthly	W/m^2	NLDAS-2 VIC Land Surface Model	(Rui and Mocko, 2018; Xia et al., 2012)
Soil Moisture	Raster-Monthly	kg/m^2	NLDAS-2 Mosaic Land Surface Model	(Mocko, 2012)
Streamflow	Hydrograph Monthly Volume	Ac-ft	NRCS Naturalized Streamflow	(Goodbody, 2020)

2023, 2021, 2019). Hence, robust explanatory and predictive models that can capture the impacts of a changing climate are crucial for efficiently managing regional water resources (Islam and Gilbert, 2024; Islam and Gilbert, 2024; Larsen et al., 2024). Several recent studies have examined the intricate connection between climate and hydrology in the URG (Islam et al., 2022; Moeser et al., 2021). While temperature and precipitation effects on streamflow often receives the primary focus (Fleming et al., 2021; Lehner et al., 2017; Moeser et al., 2021; Shultz, 2020), other hydroclimate variables may provide more specific insight into runoff processes, especially at regional scales (Trancoso et al., 2017; Xu et al., 2018) and in mountainous terrain where snowpack is a dominant water storage. Previous studies (Elias et al., 2021; Islam et al., 2022) have explored how local differences in snowpack characteristics and processes connect to variations in runoff in the URG basin; this study additionally examines the importance of streamflow predictors under recent climate change conditions.

In the western US mountains, springtime snowmelt has historically dominated hydrographs, contributing 50–80 % of the total annual

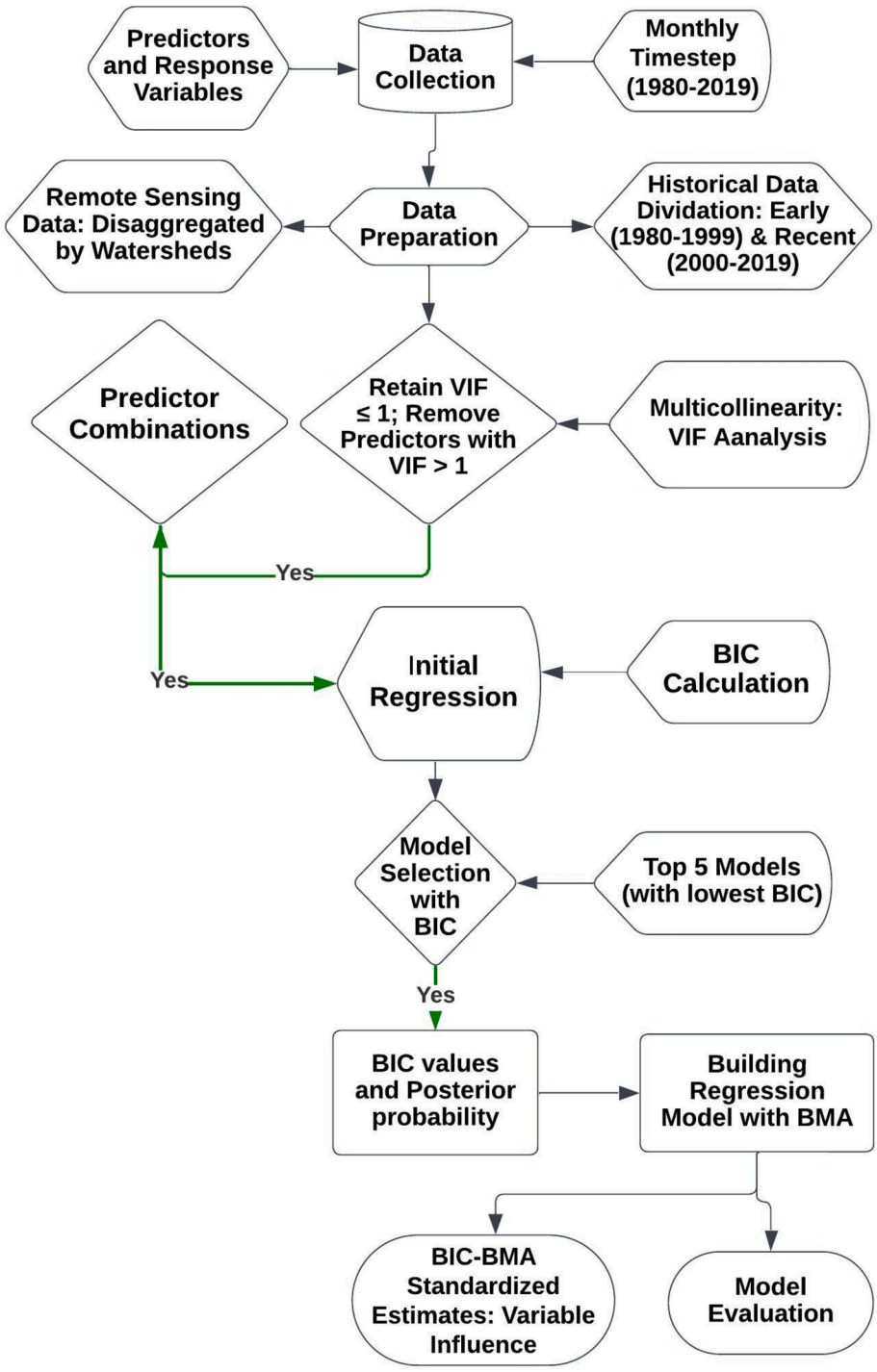

Fig. 2. Bayesian model selection and averaging across multiple models.

discharge. Recently, an increased frequency of low snowpack years has been observed, especially in areas transitioning from snow to rain dominance (Marshall et al., 2019; Steele et al., 2017), with implications for runoff amounts and timing. Variability in factors that connect watershed and hydroclimatic conditions with streamflow, such as snowpack and precipitation patterns, need further investigation, with particular emphasis on understanding how these connections have been changing. Therefore, this study investigates the importance of streamflow predictors under historical conditions as a reference for what may occur in a changing climate.

Many researchers (Amini et al., 2011; Slater and Villarini, 2017; Trancoso et al., 2017; Uwamahoro et al., 2021) have adopted integrated approaches in hydrologic analyses by incorporating regional characteristics, such as land cover, snow parameters, topography, etc., to enhance the performance of both empirical and physical models. Liao and Zhuang (2017) investigated the snowmelt factors on discharge in a spatially distributed hydrologic model – Precipitation-Runoff Modeling System (PRMS). Taia et al. (2023) explicitly addressed the spatial heterogeneity of snowmelt/accumulation parameters in hydrological models to improve snow dynamics and stream discharge estimation. Yamini R and Manjula R (2023) developed machine learning models focusing on influential parameters in the SWAT model, exhibiting improved streamflow prediction, highlighting the importance of critical drivers (R and R, 2023). Although critical for model enhancement,

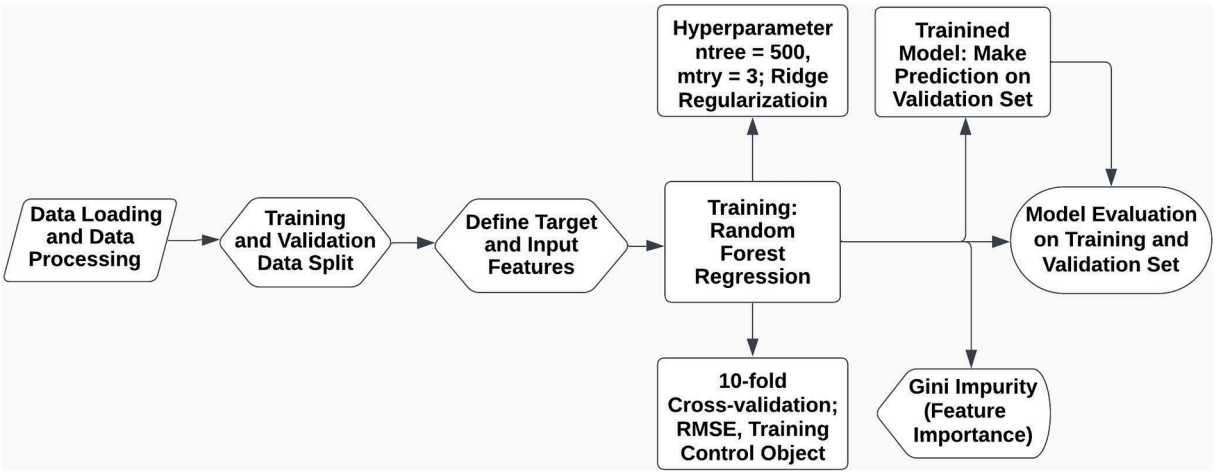

Fig. 3. Flow chart illustrating the designed process for RF analysis.

Table 3
Objective functions and their corresponding equations.

Objective functions	Equations
Index of Agreement (d)	$1-(\frac{\sum \lvert Qobs - Q\,sim\rvert}{\sum(\lvert Qobs - mean(Qobs)\rvert)+\sum(Q\lvert sim - mean(Qobs)\rvert}) \times 100$ (4)
Coefficient of Determination (R^2)	$(\frac{\sum(Qobs - mean(Qobs)) \times \sum(Qsim - mean(Qsim))}{\sqrt{\sum(Qobs - mean(Qobs))2 \times \sum(Qsim - mean(Qsim))2}})^2$ (5)
Nash-Sutcliffe Efficiency (NSE)	$1-\frac{\sum Qobs - Qsim)2}{\sum(Qobs - mean(Qobs))2}$ (6)
Bayesian R-squared (bR2)	$1-\frac{Variance\sum Qobs}{Varianceofposterior(\sum Qsim)}$ (7)

foundational studies on the key drivers for streamflow prediction in statistical models are still lacking (Islam, 2015; Islam et al., 2022; Xu et al., 2018). Assessing the relative influence of streamflow variables is essential for model simplification, integrated modeling, and multivariable calibration. Thus, the exploration of streamflow variables warrants further attention from the scientific community for its watershed modeling significance. Identifying influential variables can aid refining the empirical modeling process and guide the collection of additional data to improve predictions.

However, selecting stream variables and understanding their relative influence is complex, considering the spatiotemporal variability and process interactions that drive runoff and streamflow at the watershed scale (Islam et al., 2023; Islam and Brown, 2018; Pechlivanidis et al., 2020). Pechlivanidis et al. (2020) specifically highlighted the influence of a basin's climatology and precipitation forecast biases on the predictability of seasonal streamflow, thereby emphasizing the significance of climate-driven predictors and the uncertainties associated with their estimation. Although other studies (Islam et al., 2022; Papacharalampous and Tyralis, 2022; Pechlivanidis et al., 2020; Slater and Villarini, 2017) have discussed the importance of climate-driven variables for streamflow prediction, there are still gaps in understanding across diverse landscapes. This study addresses the gap by exploring

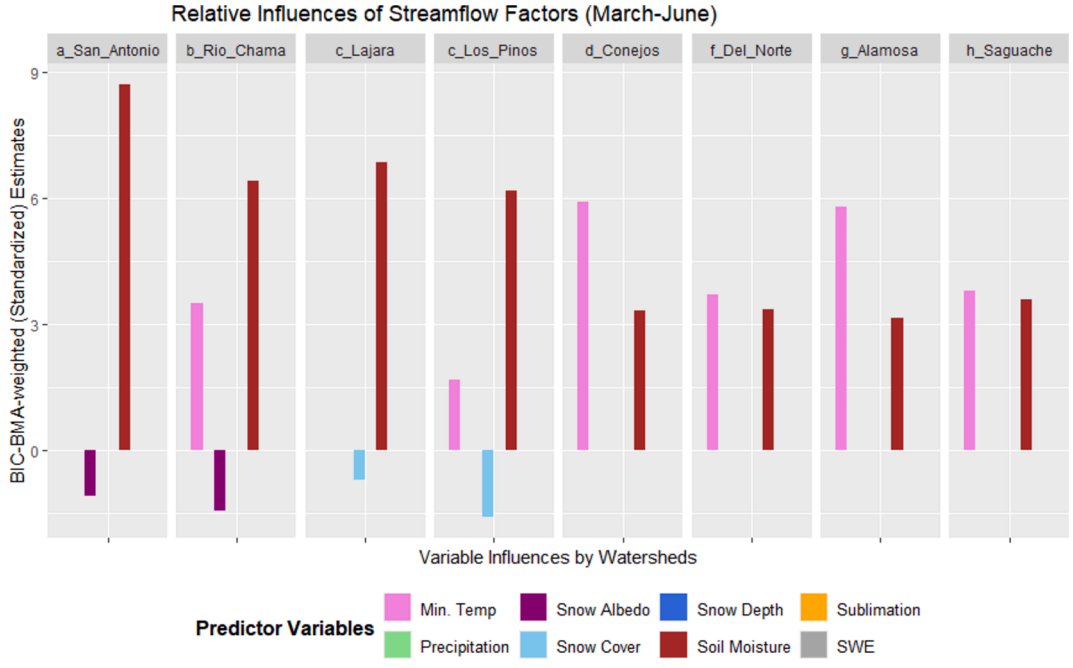

Fig. 4. BIC-BMA-weighted standardized estimates for early snowmelt and spring runoff.

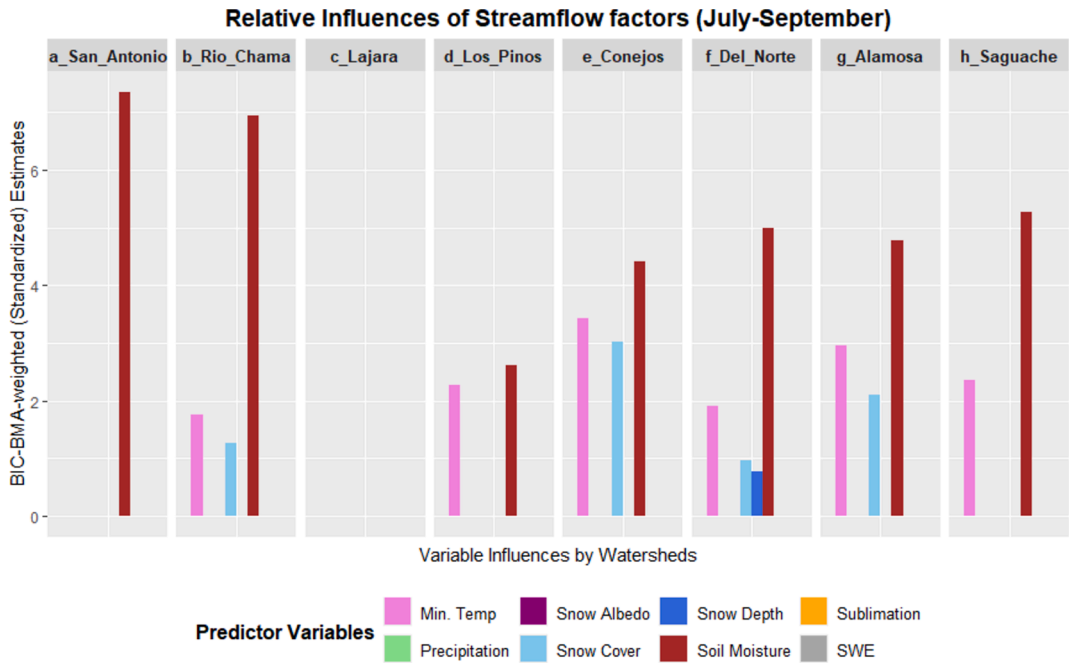

Fig. 5. BIC-BMA-weighted standardized parameter estimates for summer runoff.

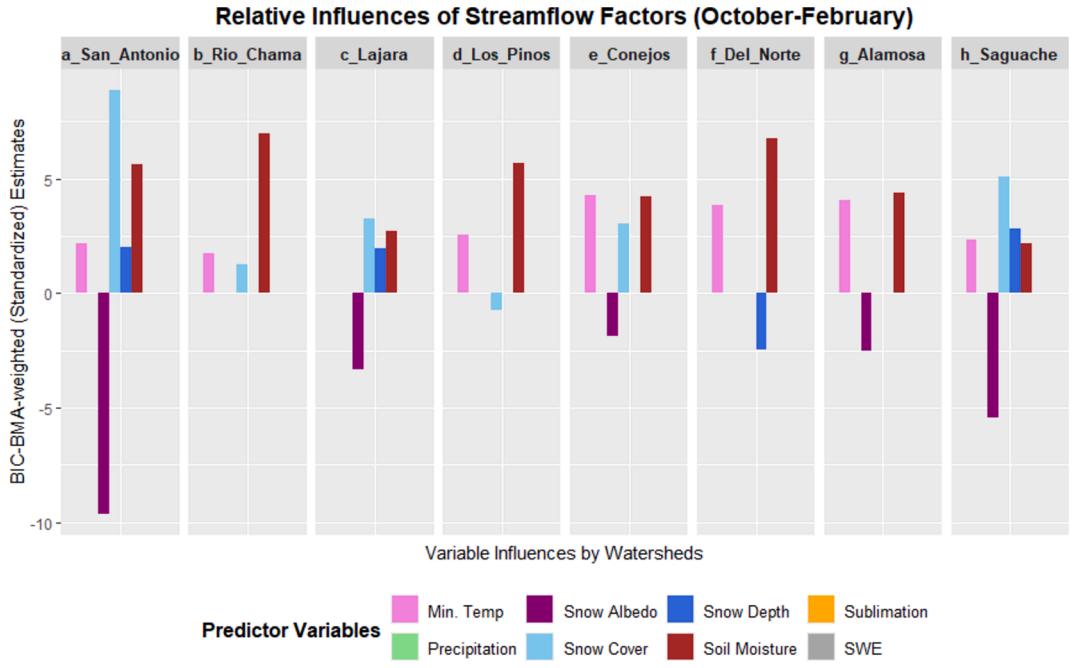

Fig. 6. BIC-BMA-weighted standardized parameter estimates for late summer and fall transition.

hydroclimate factors, their spatiotemporal variability, and the mechanisms influencing streamflow in the diverse watersheds of the URG.

In recent work, several statistical methods have been deployed to identify the most important predictors for streamflow. Slater and Villarini (2017) assessed the individual effects of predictors (precipitation, temperature, agricultural land cover, population density, and antecedent precipitation) on seasonal streamflow using Generalized Additive Models for Location, Scale, and Shape (GAMLSS) with a gamma distribution evaluated with Akaike Information Criteria (AIC). Islam et al. (2022) used AICc-weighted standardized streamflow estimates in the URG basin, mainly focusing on the importance of individual variables rather than models. However, model selection is essential for robustly addressing interacting and synergetic effects when combined variables become more influential than their individual contributions. The proposed advancement in this study involves quantifying influences emphasizing model parsimony and accounting for individual and synergistic effects. Unlike the previous studies using AIC/AICc, which are lenient in allowing more variables and sometimes lead to overfitting (Spanos, 2010), the present study prioritizes selecting models that achieve the optimal trade-off between explanatory power and simplicity, enhancing their applicability across diverse hydrological scenarios.

Bayesian Information Criteria (BIC) is considered suitable for exploring model parsimony (Huang, 2017). Both AIC and BIC are widely

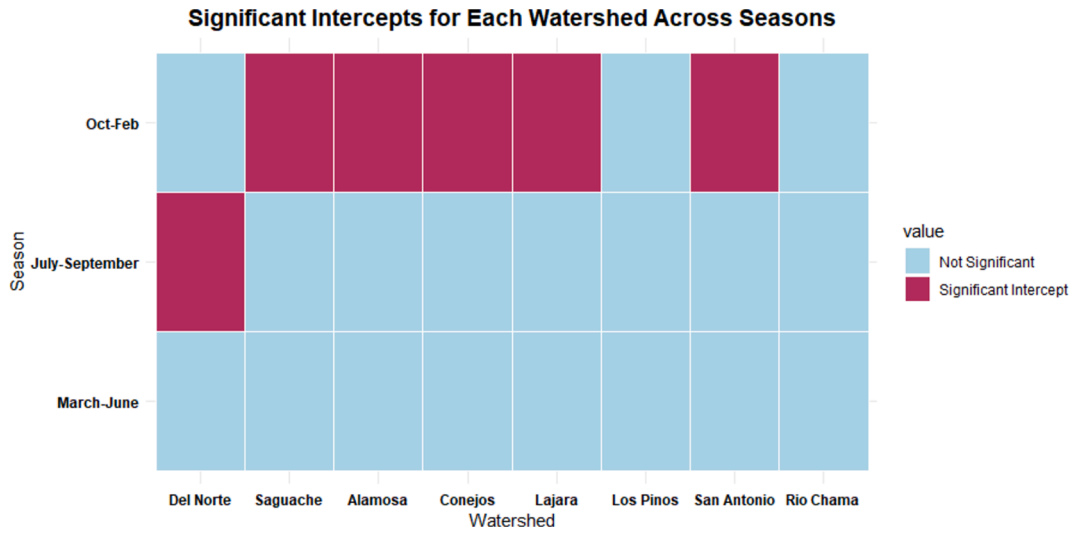

Fig. 7. Significant model intercept in seasons across watersheds.

used model selection criteria, with BIC being more consistent in choosing the parsimonious one, and it outperforms AIC, particularly in forecasting long-range scenarios (Acquah, 2010; Emiliano et al., 2014; Medel and Salgado, 2013). Emiliano at el. (2014) suggested that the BIC performed superior to the other two information criteria (AIC and AICc), especially in simulating time series models. However, the reliability of BIC-based inferences has also been questioned as it assumes a true model among candidates, which may not always be the best fit (Spanos, 2010). While BIC considers a model the best fit, complementing it with other methods can be beneficial for better accounting model uncertainties.

Bayesian Model Averaging (BMA) has been used in various domains for model development and dealing with uncertainties (Gibbons et al., 2008; Kim et al., 2020). Li (2009) used BMA to predict groundwater heads, identifying unfavorable models and propagating uncertainty. BMA has been used to enhance streamflow forecasting, as Darbandsari and Coulibaly (2020) demonstrated that the entropy-based BMA approach improved high-flow predictions (Darbandsari and Coulibaly, 2020). Zhang et al. (2009) found that BMA, combined with Genetic Algorithms, can provide reliable deterministic predictions and uncertainty analysis (Zhang et al., 2009), indicating the potential of BMA when combined with other methods. Kim et al. (2020) also showed that BMA outperformed machine learning methods with enhanced accuracy (Kim et al., 2020).

Machine learning (ML) is increasingly preferred for its simplicity in processing input data and its capacity to handle nonlinear systems in estimating variables (e.g., streamflow) (Jimeno-Sáez et al., 2022; Kim and Kim, 2021). Unlike physically based models that demand extensive information, ML provides an efficient alternative, especially when dealing with highly uncertain and complex processes. Previous studies have suggested that simple empirical models often achieve higher accuracy than process-based models (Devia et al., 2015; Islam et al., 2023), suggesting that such models provide a useful balance between model simplicity and accuracy.

This study's objectives encompass multiple approaches, including empirical model development, integrating BIC and BMA for model selection and addressing uncertainty, and identification of potential mechanisms influencing streamflow, accounting for variables' synergistic and individual effects. The developed model are validated by predicting unseen streamflow data; a secondary objective is to compare the predictions with Random Forest Machine Learning (RFML), contrasting Bayesian model-averaged regression with random forest regression (RFR). The study examines critical predictors in the RFR models, compares them with the proposed models' significant predictors, and analyzes the relative influences on streamflow.

The Bayesian methodology combining BIC and BMA is unexplored in addressing water resource problems within this URG region—a novel research scope. Additionally, the comparison with RFML expands methodological options by introducing a new approach to the study area. This study derives inferences from multiple empirical models and ensemble decision trees, to analyze critical variables and their relative importance in predicting streamflow and their spatial, seasonal, and historical variations. This study's goal of understanding how streamflow drivers are affected by a changing regional climate is foundational in projecting current and future consequences in the URG basin, an essential need for improving regional water resources planning and management.

2. Materials and methods

2.1. Site description

The domain for this study is the San Juan Mountains in the northwestern part of the URG basin, on the border of Southern Colorado and Northern New Mexico—over 1 million acres of public land in the San Juan Mountain range. The study focuses on eight watersheds delineated using USGS gauges within the mountain range. Originating in these watersheds in the San Juan mountains, the Rio Grande (RG) River flows towards the lower elevation to the southeast. This study focuses on the mountain portions of the watersheds and does not extend into the flatter San Luis Valley or the mountain ranges that form its eastern border. Fig. 1 shows the study watersheds (A) and an elevation map (B).

With an area of approximately 33,800 square kilometers, the URG basin is a vital water source for numerous communities and diverse ecosystems within the southwestern US. Flow in portions of the URG system is regulated by reservoirs and diversions operated to meet municipal and irrigation demands, impacting the natural flow patterns (USBR, 2021). The region experiences annual mean temperatures ranging from 6 to 7 °C and receives around 630 mm of precipitation, much of it falling as snow during winter (Chavarria and Gutzler, 2018). Precipitation and temperature vary across the URG basin based on latitude (36°30′ – 38°20′) and elevation above sea level. A listing of watershed properties, and associated USGS gaging stations, is shown in Table 1.

These watersheds contribute to the intricate network of rivers and tributaries that collectively shape the hydrological patterns of the study region. The region's hydrology is characterized by a snow-dominated regime, with snowmelt runoff from the upper basin contributing around 50–75 % of the RG River volume (Elias et al., 2021). The

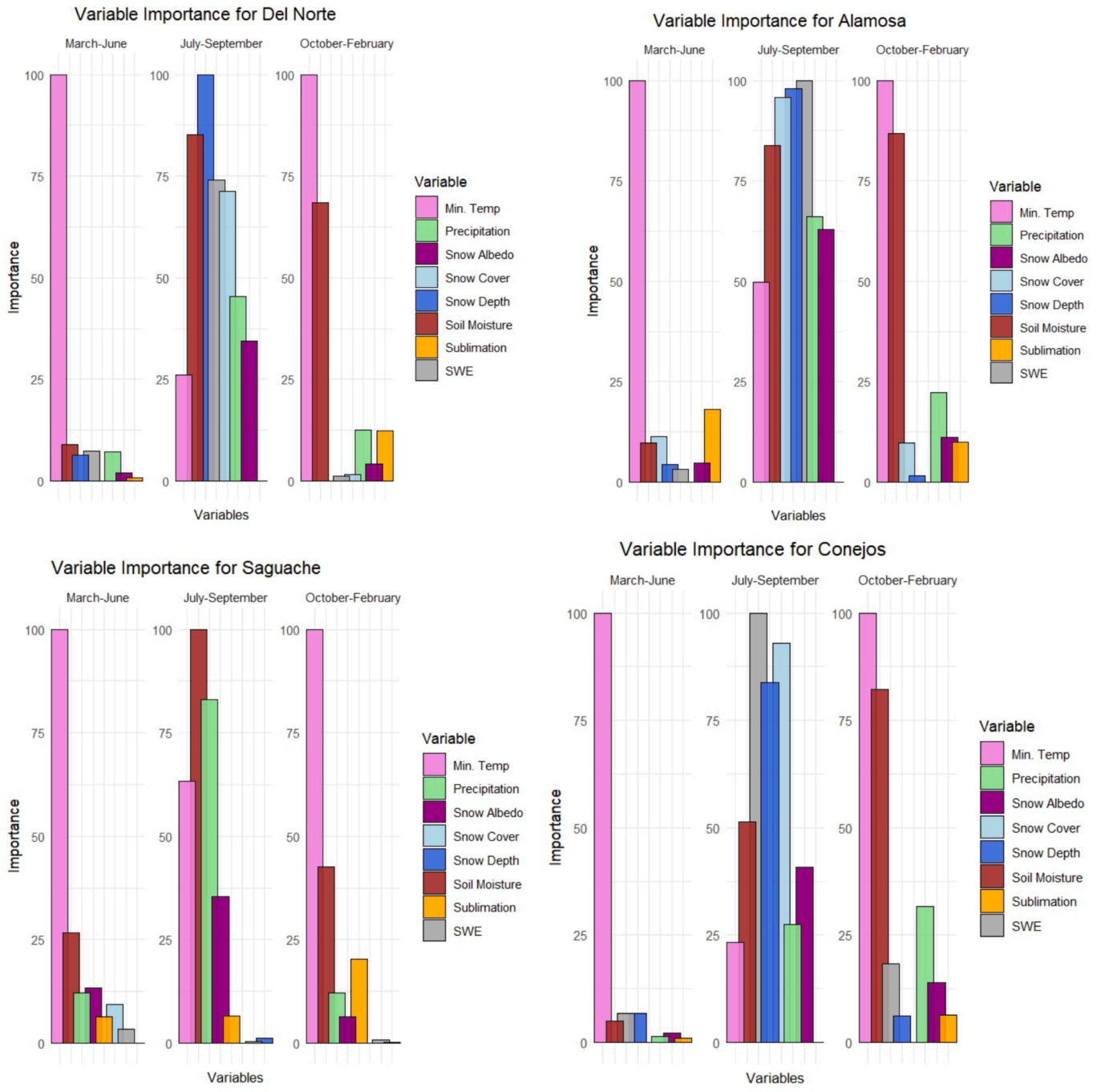

Fig. 8. RFML feature importance for Alamosa, Del Norte, Saguache, and Conejos.

watersheds comprise alpine and rugged terrain with forested slopes and lower-elevation agricultural regions. The complex landscape and topography and changing climate patterns make it challenging to simulate the watersheds' water supply system. For instance, above-average warming due to ongoing climate change is anticipated to reduce snowpack accumulation and trigger earlier snowmelt timing, affecting snowpack features like snow water equivalent (SWE), snow cover, and depth in the US Southwest, thereby impacting both the timing and quantity of runoff (Lehner et al., 2017; Marshall et al., 2019). Although peak snowpack declined from 1951 to 2015, a significant streamflow decline has yet to be seen in the URG as a rise in precipitation has compensated (Chavarria and Gutzler, 2018).

2.2. *Predictors and response variables*

This study explores a range of hydroclimate variables, including SWE, snow cover, snow albedo, snow depth, precipitation, temperature, soil moisture, and sublimation, as candidate predictors and naturalized streamflow as a response variable for time series analysis. Each of the eight predictors was selected based on evidence of their potential role in runoff generation, with an emphasis on their connection to snowpack characteristics. Other regression models for stream flow prediction have used similar variables but generally do not consider multiple snowpack properties. For instance, the Natural Resources Conservation Service method uses SWE, precipitation, temperature, groundwater levels, soil moisture, and antecedent streamflow to predict seasonal streamflow volume (Fleming et al., 2021; Garen et al., 2011).

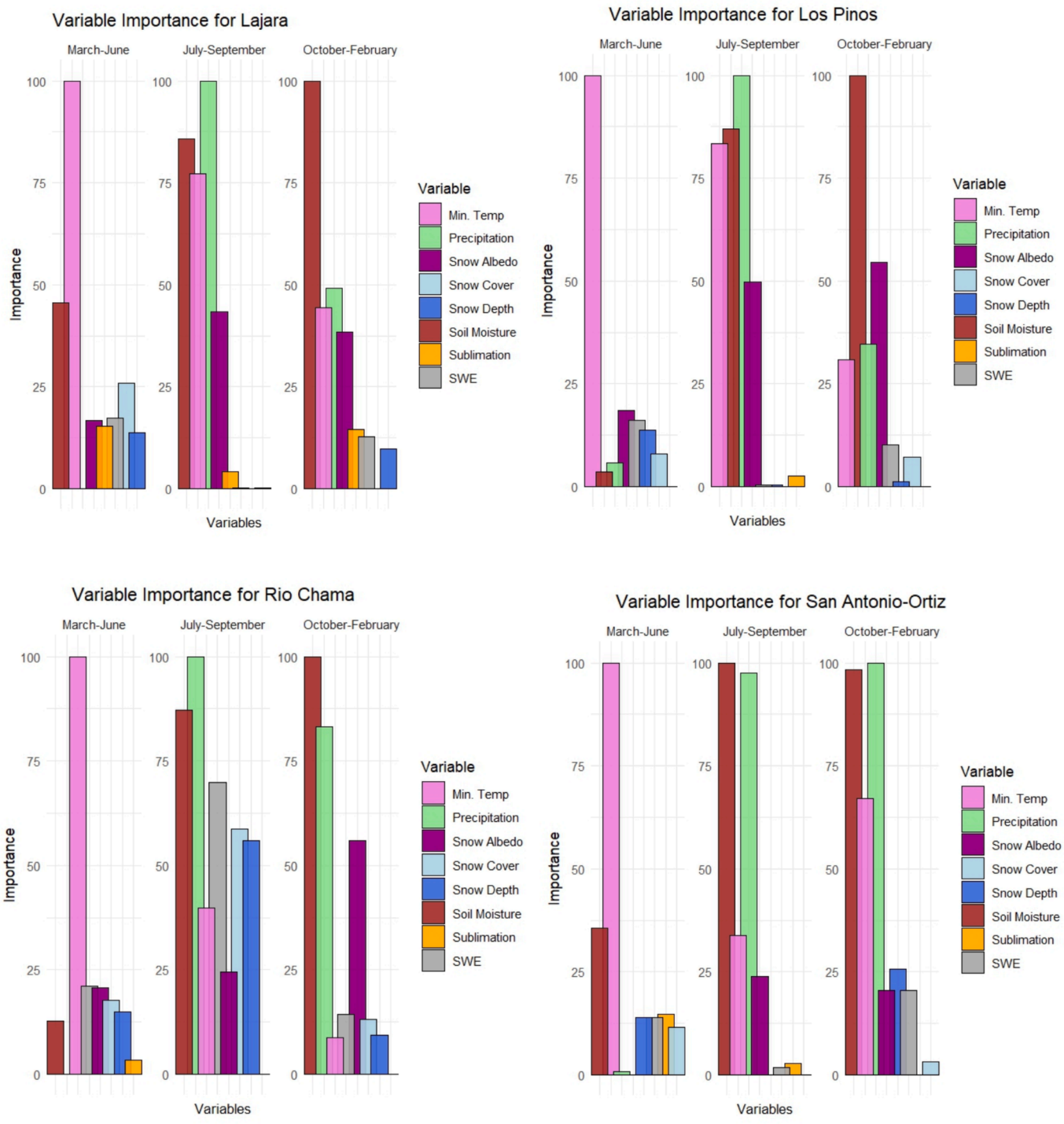

Fig. 9. RFML feature importance for Lajara, Los Pinos, Rio Chama, and San Antonio-Ortiz.

SWE is critical in predicting snowmelt runoff since its spatial variability determines the timing and extent of water supply (Schneider and Molotch, 2016). Snow cover is another crucial factor affecting snow-dominated watersheds' water supply and land–atmosphere energy balance. A more substantial snow cover cools the earth's surface by reflecting more energy, whereas a lesser amount reflects less, absorbs more energy, and heats the surface. According to Kostadinov (2019), mapping snow cover is vital for understanding snowmelt runoff hydrology (Kostadinov et al., 2019). Snow depth, another climate-sensitive indicator, can be measured in snow-covered areas. Land use and climate change-induced dryness can produce darker particles or dust that affect snow albedo, allowing more solar radiation absorption and accelerating snowmelt rates, which reduces the snow depth and consequently shortens the snow cover duration (Goldstein et al., 2016). Changes in snow albedo and increasing temperature facilitate solar radiation absorption, triggering sublimation and snowpack reduction (Lapp et al., 2005; Painter et al., 2012). Snowpack decrease and rising temperatures have already been noticed in the US Southwest; studies have recognized a strong correlation between minimum temperatures and snowmelt timing, influencing snow cover persistence and snowmelt initiation time (Islam et al., 2023; Zhang et al., 2021). Soil moisture is another important factor contributing to streamflow dynamics by joining

Table 4
Evaluation metrics for models' long-term simulation of monthly time series.

Metrics	Rio Chama		Los Pinos		San Antonio-Ortiz		Conejos		Lajara		Alamosa		Saguache		Del Norte	
	BIC-BMA	RFR	BIC-BMA	RFR	BIC-BMA	RFR	BIC-BMA	RFR	BIC-BMA	RFR	BIC-BMA	RFR	BIC-BMA	RFR	BIC-BMA	RFR
Sq-R	0.22	0.60	0.35	0.68	0.32	0.49	0.16	0.62	0.27	0.52	0.22	0.59	0.30	0.54	0.36	0.85
bR2	0.24	0.60	0.36	0.67	0.33	0.48	0.18	0.61	0.29	0.51	0.23	0.58	0.32	0.53	0.37	0.85
(d)	0.54	0.82	0.60	0.87	0.69	0.82	0.54	0.77	0.65	0.83	0.62	0.80	0.54	0.78	0.69	0.95
NSE	0.22	0.55	0.31	0.65	0.29	0.43	0.15	0.50	0.21	0.39	0.20	0.53	0.22	0.45	0.36	0.84

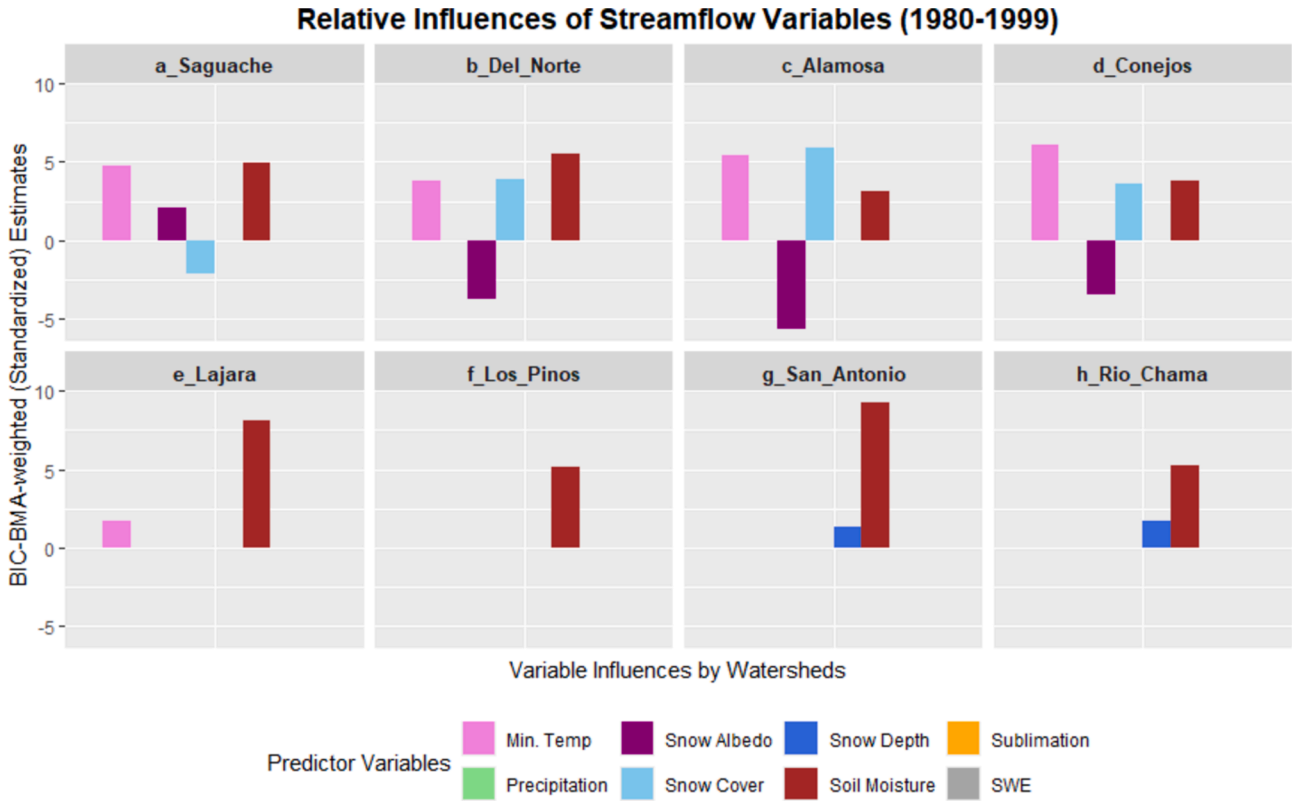

Fig. 11. Variable influence during baseline periods (1980–1999).

snowmelt runoff and precipitation input (Penna et al., 2011). Additionally, Trancoso et al. (2017) contend that soil properties significantly influence streamflow characteristics at regional scales (Trancoso et al., 2017).

2.3. Data description and preparation

Watersheds were delineated using a Digital Elevation Model (DEM) and the operational USGS gauging stations. A 30 m × 30 m resolution DEM from the Shuttle Radar Topography Mission (SRTM) was used, extracted with ArcGIS Pro 10.0, and converted to a common NAD 1983 UTM Zone 13 N coordinate system.

Advanced remote sensing techniques have improved the ability to address spatial and temporal variations in snow factors (Islam et al., 2022; Park, 2015), with common application including monitoring snow accumulation/melting variability and improve predictions (Gascoin et al., 2019; Zhao et al., 2022). This study uses long-term remotely sensed hydrologic data for the eight predictors and hydrograph data for one response variable collected in monthly time steps from 1980 to 2019 from various sites and formats detailed in Table 2.

Minimum air temperature and precipitation data are extracted from the PRSIM (Parameter-elevation Relationsships on Independent Slopes Model) (Daly et al., 1997). The PRISM data is produced through is a spatial modeling technique that estimates climatic variables utilizing weather stations' point measurements, digital elevation data, and other spatial information (Liu et al., 2019) combined through regression relationships to generate gridded datasets at high spatial resolutions. The PRISM model applies regression relationships between climate variables and geographic features to generate gridded datasets at high spatial resolutions, enhancing regional climate patterns' spatial understanding (Lehner et al., 2017; Strachan and Daly, 2017). A study by Lehner et al. (2017) successfully used the PRISM data for precipitation and surface air temperature in the URG region.

Estimates of snowpack characteristics are obtained from the NLDAS-2 datasets. NLDAS (North American Land Data Assimilation System) assimilates observational data from various sources, including ground-based stations and remotely sensed satellites, to create high-quality land surface models and datasets for North America (Daly and Bryant, 2013). Researchers studying land surface modeling and hydrology often rely on NLDAS-2 data (Tran et al., 2022).

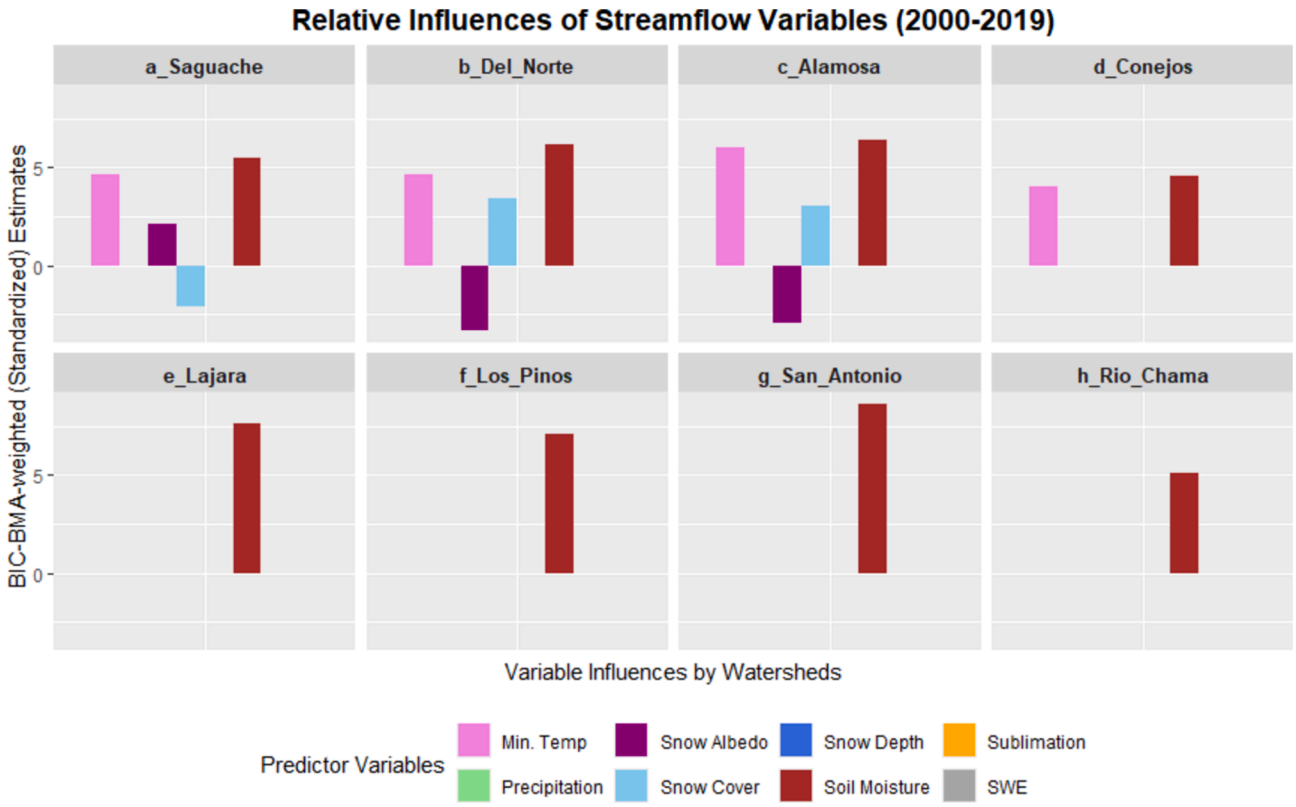

Fig. 12. Variable influence in the recent periods (2000–2019).

We used naturalized streamflow (monthly volume) adjusted by the Natural Resources Conservation Service (NRCS). The NRCS adjusts streamflow volumes recorded at gages to account for regulations like reservoir storage and direct diversions (Goodbody, 2020; Islam et al., 2022); this eliminates water management effects and allows a more accurate study of hydroclimatic effects alone.

2.3.1. *Raster data synthesis*

The PRISM and NLDAS-2 data, originally at spatial resolutions of 4 km × 4 km and 0.125 degrees (~14 km), respectively, were obtained as gridded rasters at a monthly time step. These initial monthly raster cells were disaggregated into a 30 m × 30 m resolution to match the DEM (as standard), followed by clipping into the sub-watershed border, which allows for capturing finer watershed boundaries and can improve spatial consistency in areas with complex terrain. Watersheds' monthly responses were then calculated by averaging disaggregated pixels as monthly mean values for the variables of interest. So, each watershed has a single monthly value, which is used to make up the time series. All the data processing and analyses were performed in the RStudio interface (Allaire, 2012); the raster package's "disaggregate()" function was used in raster resampling, utilizing bilinear interpolation of the nearest neighbor method (Hijmans et al., 2023).

2.4. *Seasonal and historical divisions*

Most of the URG's annual streamflow typically occurs during spring and early summer, driven by snowpack melting (Chavarria and Gutzler, 2018; Islam et al., 2022). Climate change has altered runoff patterns, increasing in winter flow while decreasing in summer. Elias et al. (2021) observed that the runoff shifts from June-July to April-May in a warmer climate affects streamflow timing from March-April to mid-May and throughout the year. Pechlivanidis et al. (2020) emphasized the importance of the initialization month and the prior knowledge of local hydroclimatic conditions in predicting seasonal streamflow (Pechlivanidis et al., 2020). Considering this, this study divides the water year into three seasons to evaluate these seasonal changes, and it categorizes long-term data into baseline or early periods (1980–2000) and recent periods (2001–2019). Splitting the historical record in this way was done to facilitate comparison across periods and to aid in identification of factors influencing hydrologic regimes.

Based on the URG local hydrological and climatic conditions, the water year is divided into three seasons: 1. "Early Snowmelt and Spring Runoff" season (March-June), experiencing increased streamflow due to early spring snowmelt, 2. "Summer Flow" (July-September), which represents stable and relatively high streamflow post-peak snowmelt, and 3. "Late Summer and Fall Transition" (October-February), which transitions from summer flow to snowpack building for next year, when streamflow decreases as temperatures drop and snow accumulation begins.

2.5. *Analytical approach*

A linear regression framework tests the influence of different combinations of the eight predictor variables on fitting the monthly naturalized streamflow record. Bayesian information criteria (BIC) and Bayesian model averaging (BMA) are used to discern the impacts of these predictor variables on seasonal and annual components of streamflow while creating a composite regression model; this regression framework is referred to here as the BIC-BMA model. The study analyzed seasonal and long-term changes in streamflow generation mechanisms and identified emergent variables influencing streamflow. The water year was segmented into three seasons to analyze the variability of these impacts throughout the annual cycle. Historical data is divided into early and recent periods, enabling the identification of variables affecting streamflow across two separate climate periods. We evaluated the significance of the predictor variables in the BIC-BMA model and used the Gini feature importance within RFML to understand better the factors driving the influences. Model fitting (regression and RFML) and

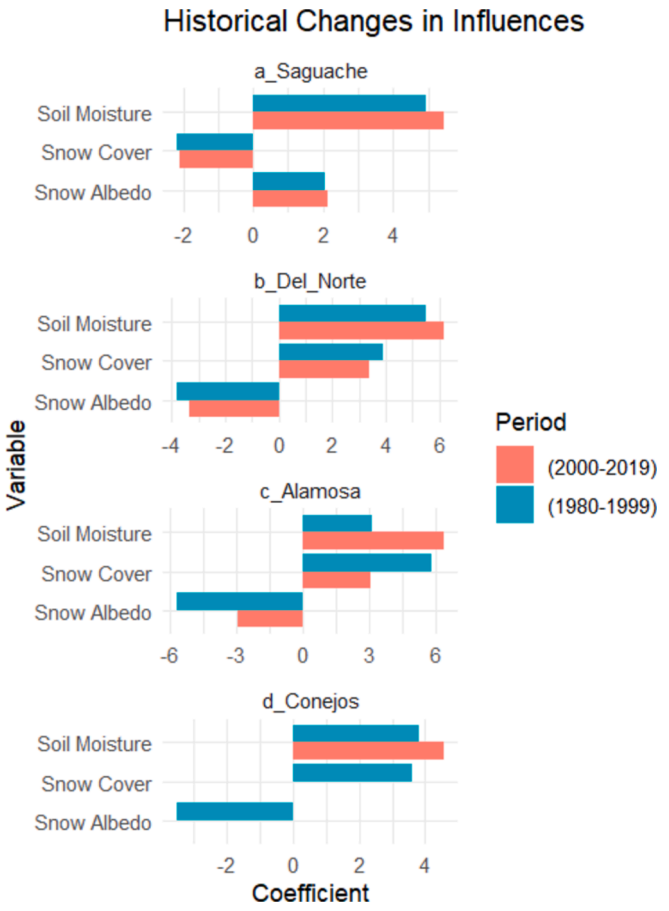

Fig. 13. Historical changes in influences for three important predictors.

monthly time series (1980–2014) simulation were performed to assess models' overall prediction accuracy, validated by unseen streamflow (2015–2019). The study thoroughly examined how hydroclimate variables affect streamflow in a changing climate, incorporating seasonal, historical, linear, and nonlinear assessments.

2.5.1. *Bayesian analyses: Bayesian model selection and averaging*

Bayesian Information Criterion, BIC, is a statistical metric used for model selection. It assesses and compares models to determine the optimal based on parameter quantity and goodness of fit. BIC is calculated using the formula

$$(\mathrm{BIC}) = -2 * \text{log-likelihood} + k * \log(n) \quad (1)$$

where "log-likelihood" evaluates model-data fit, "k" is the number of parameters, and "n" represents the number of data points (streamflow observations). The model with the lowest BIC value is considered the best, reflecting a balanced between model fit (indicated by likelihood) and model complexity (penalized by parameter count)(Neath and Cavanaugh, 2012). Unlike AIC/AICc, BIC typically places a stronger penalty on model complexity and becomes more conservative in selecting simpler models (Emiliano et al., 2014; Medel and Salgado, 2013; Weakliem, 1999). From multiple candidate models, BIC selects the most parsimonious model that adequately explains the variations in the target variable, emphasizing simplicity while penalizing complex models to prevent overfitting (Huang, 2017). It is typically suitable when data points significantly outnumber variables (Kim et al., 2023), aligning with this study. BIC assumes a "true model" among candidates—a strong assumption, and its stricter penalty for complexity may lead to underfitting. While BIC prioritizes simpler models, penalizing complexity inherently introduces uncertainty because the actual model might be more intricate. Thus, BIC may not capture the inherent uncertainty, especially when dealing with real-field data where the underlying model may be uncertain.

BMA is another approach that directly addresses model uncertainty by assigning prior probabilities and calculating posterior model probabilities, providing a probabilistic framework for model selection (Gibbons et al., 2008; Kim et al., 2020; Robertson and Wang, 2009). Instead of relying solely on a model with the lowest BIC value, the study adopts a model-averaging approach that considers a range of plausible models to cover diverse perspectives. The model averaging approach allows these multiple models – a source of uncertainty – to be incorporated into a single prediction. The formula (2) represents the BMA-predicted outcomes (Y),

$$Y = \Sigma_{i=1 \text{ to } m} W_i (\beta_{0i} + \beta_{1i}X_1 + \beta_{2i}X_2 + \ldots + \beta_{pi}X_p) \quad (2)$$

Y is calculated by adding up the products of weights assigned (Wi) and the coefficients for intercept and predictors (β_{0i},β_{1i},…,β_{pi}) from each model. The predictors are denoted as X_1, X_2…Xp, where p is the total number of predictors. Summation is taken over i models, where m represents the total number of models considered. In the BMA context, BIC is used to assign weights to the models based on their balance of fit and simplicity, i.e., models with lower BIC (a better balance of fit and simplicity) receive higher weights and thus contribute more to the model-averaging process.

2.5.2. *Proposed model: BMA based multilinear regression*

The process begins with defining predictors and response variables. Some predictor variables may have a strong correlation with each other. Therefore, the procedure accounted for multicollinearity by assessing Variance Inflation Factors (VIF). Using the 'vif' function from the 'car' package (Fox et al., 2007) and removing variables with VIF > 1, the study addresses the multicollinearity issue—a standard practice. The VIF values greater than one indicate correlated predictors contribute to unstable regression coefficients and inflated standard errors (Gregorich et al., 2021). Model building involves generating all combinations of eight predictors ($2^8 - 1$) for the top model, and the BIC is computed for each model. Since log-likelihood contributes to the BIC calculation, the top 5 models, ranked by the lowest BIC, are selected to prepare a design matrix of predictors and response variables for subsequent BMA analysis. While including more models in model averaging (BMA) could theoretically improve robustness, models with higher BIC values contribute less to the results because they are assigned lower weights. Therefore, considering all possible combinations without prioritizing BIC would undermine the reliability of using BIC as a model selection criterion, and it would lead to including many suboptimal models, thereby diluting the strength of the best models. Increasing the number of included models beyond 5 did not lead to qualitatively different results but made interpretation more difficult. We balanced the model overfit and the uncertainty by focusing on the top 5 models with the lowest BIC in model average estimates. The 'BMA' package is used to analyze and extract the best model using BMA (Amini and Parmeter, 2011). The 'bicreg' function of the 'BMS' package considers multiple models in assimilating the best model based on the BIC. Standardized coefficients in the BIC-BMA regression model are calculated and used as the primary metric to assess the relative importance of each predictor. It quantifies the influence of each predictor variable on streamflow, considering the differences in scale. Standardized coefficients, or beta coefficients, represent how much the response variable (dependent variable) changes in standard deviation (SD) for each SD change in the predictor variable (independent variable). A higher standardized coefficient signifies a greater impact on the response variable (streamflow); positive coefficients mean that an increase in the predictor is associated with an increase in streamflow, while negative coefficients represent inverse relationships. The model is then used to make predictions of unseen streamflow data (years 2015 – 2019, not used in the model

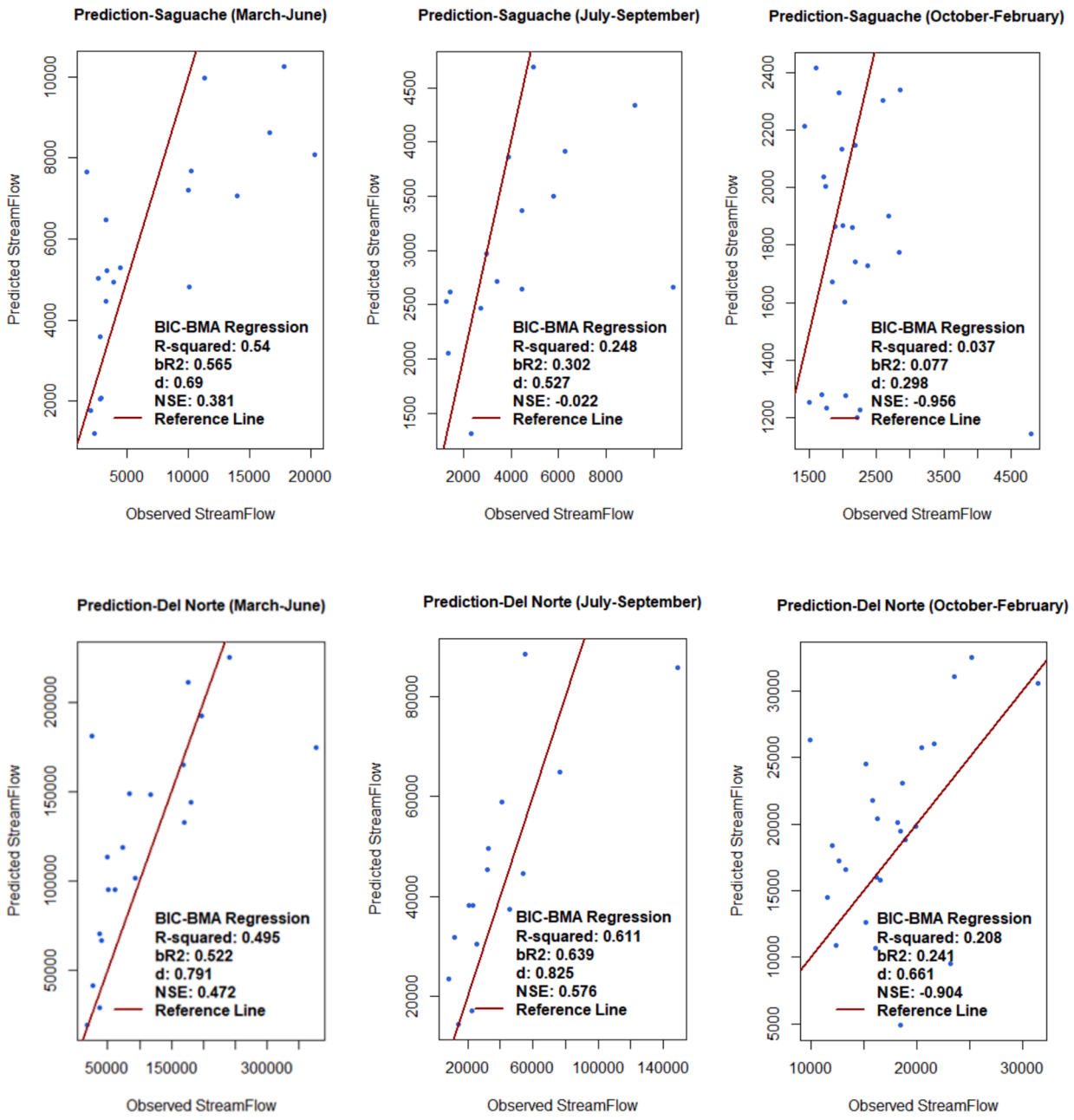

Fig. A1. BIC-BMA regression model Scatterplots for seasonal prediction.

fitting) based on new data on the predictor variables. Fig. 2 shows the proposed model's procedural flowchart.

2.6. Forest-based predictive modeling

Random forest machine learning (RFML), a supervised ML method, uses ensembled decision trees to improve predictive performance and reduce overfitting. Ensemble learning is a technique that trains each tree on a random subset of the data at each split (Breiman, 2001), allowing it to de-correlate the individual trees and enhance the model's generalization capability. The algorithm aggregates the forecasts from individual decision trees to generate a final prediction. Regarding accuracy estimation, RF has an internal mechanism for estimating the out-of-bag (OOB) errors that assess the model's ability to generalize for unseen data by evaluating the performance of each tree on the data points not included in the training subset. The aggregated OOB errors across all trees provide an overall accuracy estimate (Breiman, 2001; Svetnik et al., 2003).

2.6.1. Gini feature selection

Gini impurity measures feature importance, counting each feature's contribution to reducing variance (or "impurity") across decision trees, (Archer and Kimes, 2008; Dewi and Chen, 2019), which is a key criterion in RF for splitting nodes into individual trees. Gini impurity measures the likelihood of misclassifying a randomly selected element in a dataset, and it is used in decision trees as a component of a random forest. Gini impurity is calculated using class probabilities, defined by the formula:

$$\text{Gini}(S) = 1 - \sum_{i=1}^{c} (p_i^2) \quad (3)$$

where S is the set of data points, c is the number of classes, pi is the

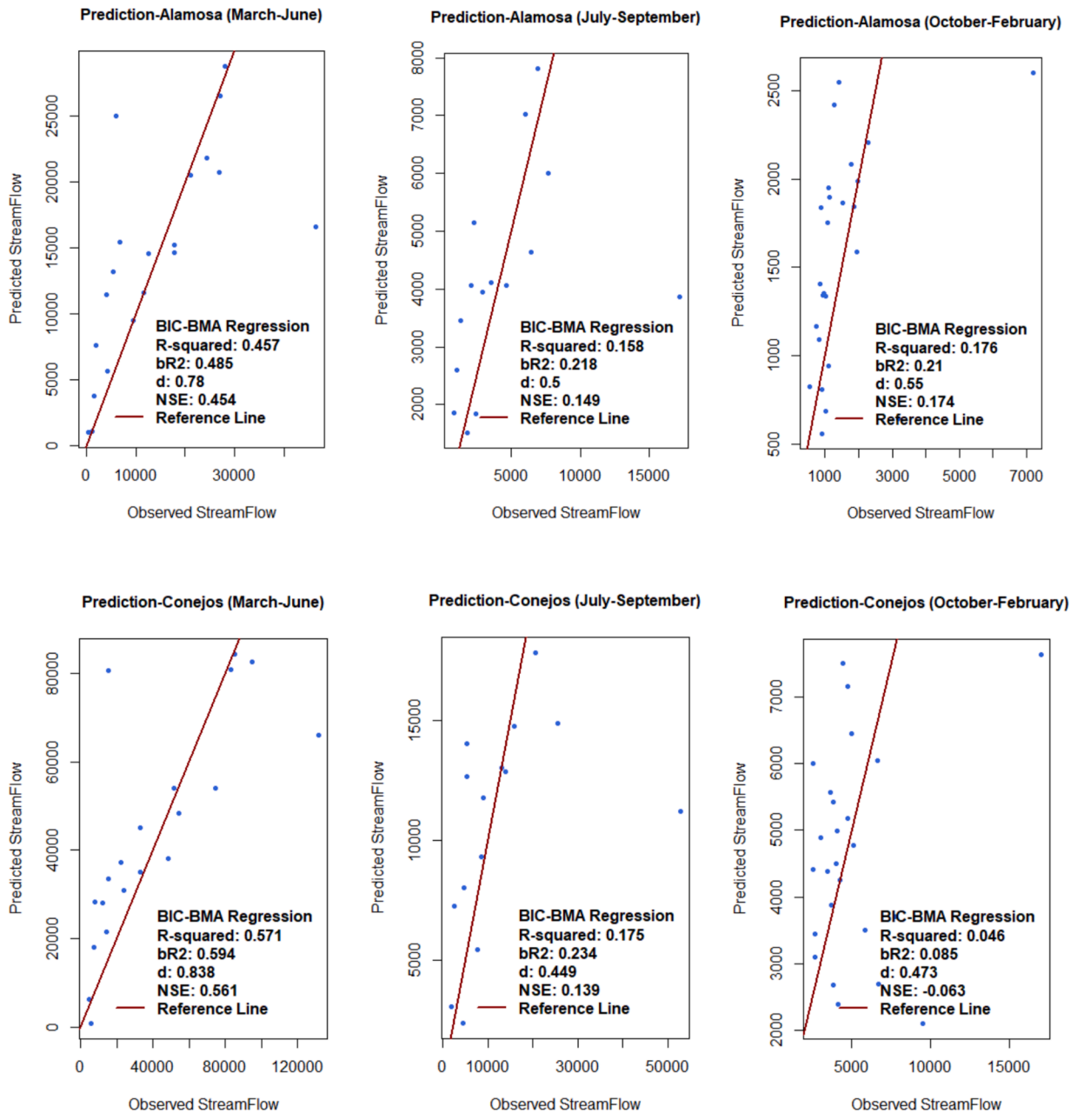

Fig. A1. (*continued*).

probability of selecting a data point of class i from set S, and where pi = (Number of data points with class i) / (Total number of data points in set S). In random forest regression (RFR), the algorithm similarly measures each feature's contribution to reducing variance (or "impurity"), known as Mean Decrease in Impurity (MDI). The MDI averages impurity reduction across all trees in a forest and indicates variable importance, which allows variables to be ranked based on their influence on the model's predictions (Scornet, 2023). In R's 'randomForest' package, the 'varImp' function provides variable importance as a percentage; a higher percentage value indicates greater importance, contributing more to accuracy.

2.6.2. *RFR – Random forest regression*

Random Forest Regression (RFR) is a variant of RFML, able to predict continuous values (Liu et al., 2020). Comparative studies showed the superiority of RFR over other machine-learning algorithms and traditional statistical methods in streamflow prediction, especially in regions characterized by intricate hydrological processes and limited data availability (Jimeno-Sáez et al., 2022; Liu et al., 2020; Schoppa et al., 2020; Virro et al., 2022). RFR captures the nonlinear relationship between predictors and response variables since it does not rely on the linearity assumption, making it more robust to collinearity than other regression methods (Li et al., 2020; Ma and Cheng, 2016). RFR has also been applied in streamflow predictions, specifically in successfully predicting hydrographs in snowmelt driven watersheds (Cho et al., 2019).

2.6.3. *Designed algorithms for RF analysis*

The 'randomForest' package (RColorBrewer and Liaw, 2018) was used to build the RF regression model. The monthly streamflow and predictor variable time series dataset described earlier is used as input to the RF regression model. Bootstrapping and out-of-bag (OOB) sampling are used to expand the dataset size for training. Hyperparameter optimization is performed via random search over a space defined by *ntree*

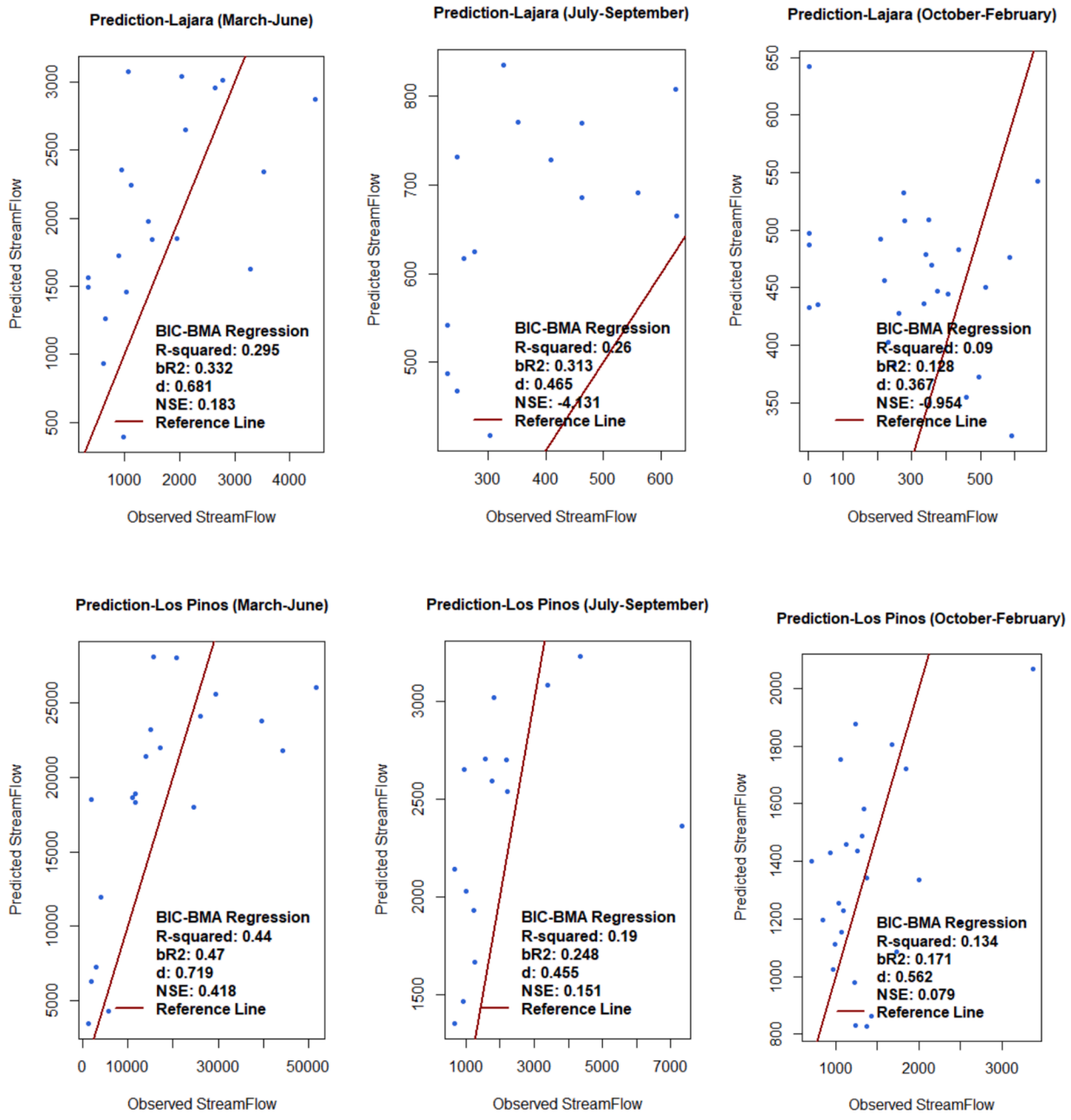

Fig. A1. (*continued*).

(number of trees = 500), *mtry* (variables randomly selected at each split = 3), and *maxnodes* (maximum terminal nodes). *mtry* is usually recommended to be one-third of the feature number in RFR and *ntree* to be 500 as a standard (Breiman, 2001; Hastie et al., 2001; Liaw and Wiener, 2002). Root Mean Square Error (RMSE) is the training control object for 10-fold cross-validation (method = 'cv,' number = 10). Ridge regularization adds a penalty term to control model complexity and addresses overfitting during training (Hoerl and Kennard, 1970). Although Random Forests inherently addresses overfitting through ensemble and bootstrapping, intentionally incorporating ridge regularization can benefit specific datasets, providing an additional layer of control over the model complexity. While not a standard feature of the 'randomForest' package, the effectiveness of its inclusion is monitored on training and validation data. If the model generalizes well and avoids underfitting, ridge regularization would be a valid strategy. The 'caret' package automatically selects the best hyperparameter combination based on the minimum RMSE value. The resulting model, trained on the entire dataset, provides an overall performance estimate (i.e. a measure of how well the model estimates streamflow based on selected predictor variables). Evaluation metrics are calculated for each fold during cross-validation, and all folds are then averaged. Finally, the trained model is tested on a separate validation data set (i.e., not utilized in bootstrap and out-of-bag) for streamflow prediction. Fig. 3 depicts a procedural flowchart of the RF analysis as designed.

2.6.4. *Linear vs. Nonlinear approach*

Hydroclimate drivers and streamflow exhibit diverse relationships that vary spatially and temporally. The BIC-BMA model highlights linear aspects of the relationship, balancing model fit and complexity while addressing uncertainty through probabilistic insights into the drivers' relative importance. Standardized coefficients derived from BIC-BMA-based model quantify streamflow impacts, making the influence of each driver of streamflow comparable across scales and units. Despite the nonlinearity of rainfall-runoff processes at certain scales, the

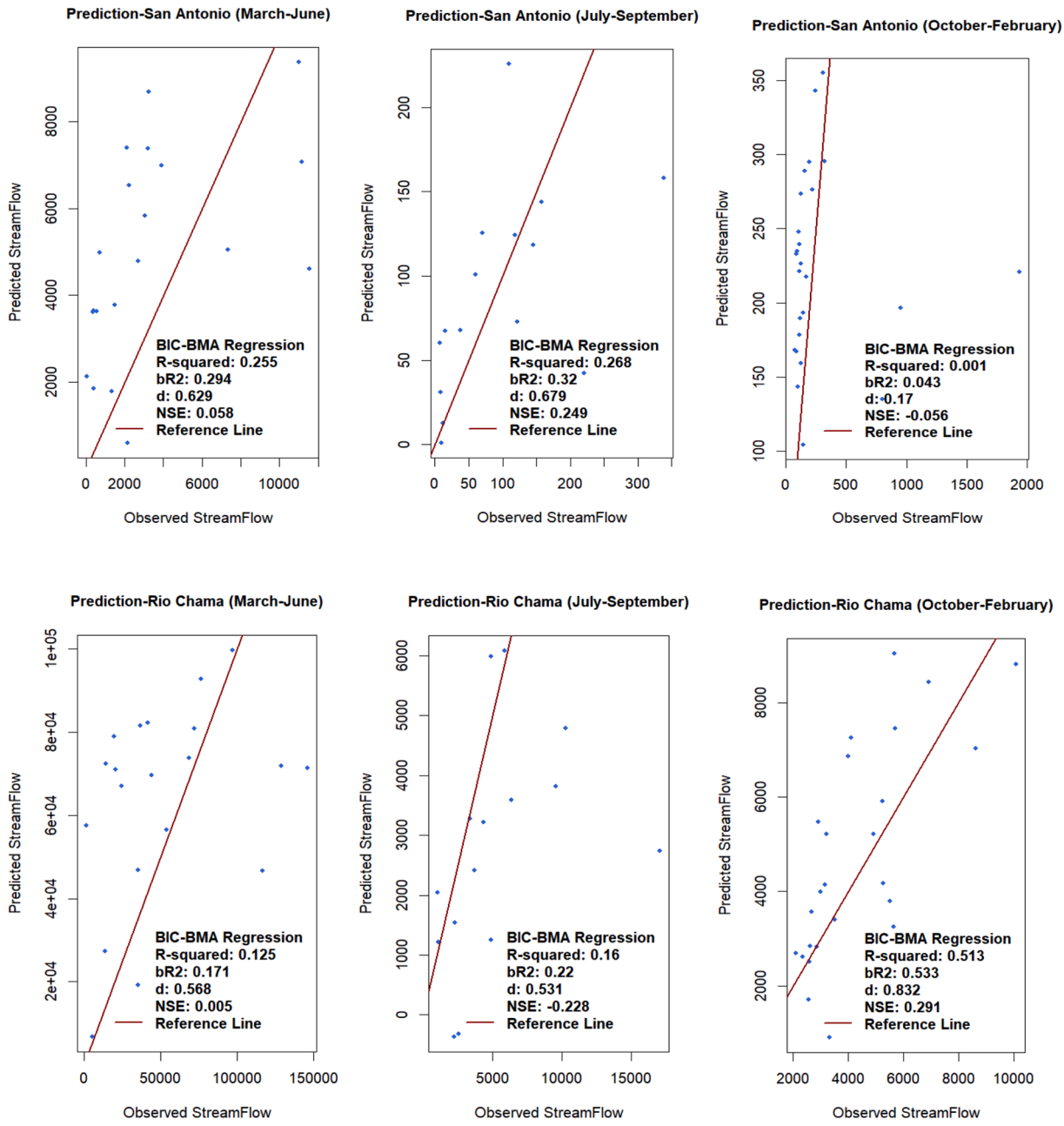

Fig. A1. (*continued*).

linearity assumptions underlying the BIC-BMA are analogous to those employed in the many regression-based operational flow and water supply forecast methods that have been used across the Western United States for many decades (Garen, 1992; Rosenberg et al., 2011).

On the other hand, RFR, an ensemble ML method, captures nonlinear interactions and handles diverse data and multicollinearity (Archer and Kimes, 2008; Grömping, 2009); RFR incorporates bootstrapping for uncertainty and provides out-of-bag accuracy estimates, which expose another insight that complements BIC-BMA and helps identify discrepancies arising from linear assumptions. Together, these models leverage their strengths—BIC-BMA for interpretability and quantified impacts and RFR for capturing more complex nonlinearities—to provide a comprehensive understanding of streamflow sensitivities across spatial and temporal scales.

2.7. Performance metrics

Table 3 presents error metrics to evaluate models' predictive performance from various perspectives. R-squared explained variance (Islam et al., 2015; Leta et al., 2018), while Bayesian R-squared (bR2) incorporates parameter uncertainty through posterior distributions (Gelman et al., 2019). The index of agreement (d) measures both mean differences and variability. Nash-Sutcliffe Efficiency (NSE), another widely used metric in hydro-modeling, assesses how closely model predictions align with observed variability. Together, these metrics provide complementary insights into model fit for streamflow prediction.

Here, Qobs is observed, and Qsim is the predicted streamflow. Optimal performance for R-squared, bR2, NSE, and d is typically achieved with values close to 1. Satisfactory performance for NSE is generally indicated by values greater than 0.5. Ideally, R-squared and bR2 should exceed 0.5, while the d should fall above 0.4 for satisfactory

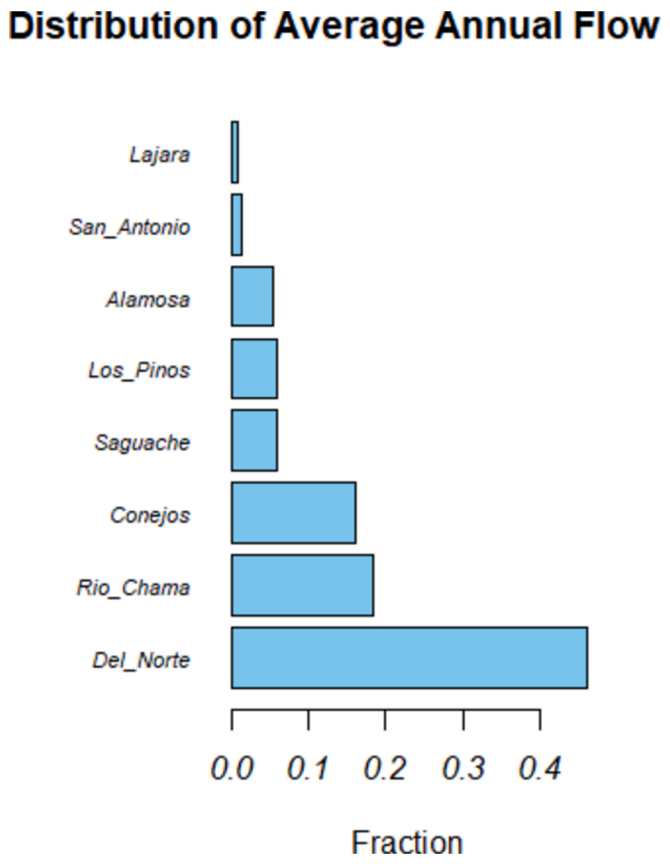

Fig. B1. Fractional distribution of annual average streamflow.

performance (Hussainzada and Lee, 2021; Senent-Aparicio et al., 2021).

3. Results

3.1. Seasonal analysis

The BIC-BMA weighted standardized parameter estimates are used to determine the predictor influences; a higher value of the standardized coefficient indicates a more substantial effect on streamflow. BMA assigns posterior probabilities to the entire set of coefficients; these probabilities describe the likelihood of a variable being included in the model while considering all coefficients, which allows uncertainty to be addressed. The parameter estimates are obtained using BMA, where BIC-based weights are assigned to different models (BIC-BMA Models, Supplementary Table); estimates are then standardized. Figs. 4, 5, and 6 present key predictors and their influences (1980–2014) on streamflow across three seasons (March–June, July–September, October–February) by watersheds, ordered from left to right by elevation, with the lowest elevation watershed on the left and the highest on the right. These figures showed the predictor variables with a posterior probability above 20 %; predictors with a posterior probability below 20 % are omitted from the BIC-BMA-weighted standardized illustrations.

In March-June, a soil moisture and minimum temperature significantly influenced streamflow (Fig. 4) across most watersheds. For San Antonio, the standardized coefficient for soil moisture is 8.71; it means that a one standard deviation SD rise in the soil moisture is associated with an 8.71 SD increase in the streamflow response. Minimum temperature is the most influential variable for Alamosa, Del Norte, Saguache, and Conejos (northern latitudinal and high-altitude watersheds) in this early snowmelt and spring runoff.

Figs. 5 and 6 also highlight the significance of soil moisture from July to February (July–September and October–February), identifying it as a key predictor across watersheds. However, the impact scores of soil moisture generally decrease in October-February (Fig. 6: late summer and fall transition) compared to the other two seasons. During late summer and fall transitions, snow accumulation and freezing temperatures may affect the relationship between soil moisture and streamflow, delaying water infiltration and its immediate contribution to streams.

Snow albedo plays a significant role in streamflow dynamics from October to February, interacting with other factors, i.e., minimum temperature, snow cover, and soil moisture. Negative snow albedo values observed during this period (Fig. 6) indicate increased reflection of solar radiation, contributing to surface freezing and reducing streamflow generation in these months. The Lajara watershed had no predictor (Fig. 5) because all predictors' posterior probability is below 20 %. In some cases, the model intercept becomes statistically significant either on its own or in conjunction with other variables – a situation where predictor coefficients may be zero, but streamflow is nonzero; it suggests that the model predicts a non-zero value even when all predictor variables are zero. A significantly positive intercept could imply that a significant portion of streamflow originates from sources not explicitly accounted for in the model, such as groundwater or baseflow, or carryover effects from other watershed stores. Fig. 7 shows the significant model intercepts across watersheds in three seasons where this occurs.

The intercept is notably significant in late summer and the fall transition (Oct-Feb), with the Del Norte being exclusively significant in summer flow. The Del Norte watershed is characterized by its unique nature – diverse elevation, extensive watershed area, and low-lying agriculture; it has been previously cited for early snowmelt runoff issues (Islam et al., 2023). In contrast, Los Pinos and Rio Chama watersheds, situated in the southernmost part do not show model intercept significance.

The RFR analysis of predictor importance at seasonal scales shows similar results. The Gini impurity measure of RFR confirmed minimum temperature as the key predictor for March-June across all watersheds (Figs. 8 and 9).

Fig. 8 indicates that minimum temperature consistently has the highest impact in March-June across watersheds, outweighing other predictors. However, soil moisture also remained significant for the San Antonio and Lajara watersheds.

During October-February (Fig. 6 & Fig. 9), soil moisture becomes more influential across watersheds, emerging as a top predictor in both the BIC-BMA and RFR analyses, especially in the lower elevation watersheds in the southern part of the San Juan Mountains. Interestingly, the RFR method identifies more important predictors in the July-September season, suggesting a more complex streamflow generation process. Specifically, precipitation and snow parameters have increased in importance during this period compared to the other seasons. In higher elevated areas (Fig. 8) like the Del Norte, Alamosa, and Conejos, snow-related factors such as SWE, snow depth, and snow cover significantly influenced streamflow. In contrast, precipitation emerges as the significant predictor for lower elevated watersheds (Fig. 9) like Lajara, Rio Chama, Los Pinos, and San Antonio-Ortiz. Appendix A compiles scatter plots for seasonal predictions, comparing predicted vs. observed streamflow.

The analysis results suggest that predictive accuracy is typically higher during March-June than in other seasons, except in Del Norte and Rio Chama, the top two watersheds in terms of streamflow volume (Appendix B). The RFR models show stable performance in March-June, as indicated in RF validation/cross-validation tables (Performance Matrices, Supplementary Table). BIC-BMA-based regression models demonstrated comparable performance to RFR at the seasonal time scale, with some instances of superior performance. However, RFR consistently outperforms in cases where intercepts were significant. This superiority is attributed to RFR's enhanced capability to capture nonlinear effects, including delayed impacts such as the gradual release of water from snowmelt.

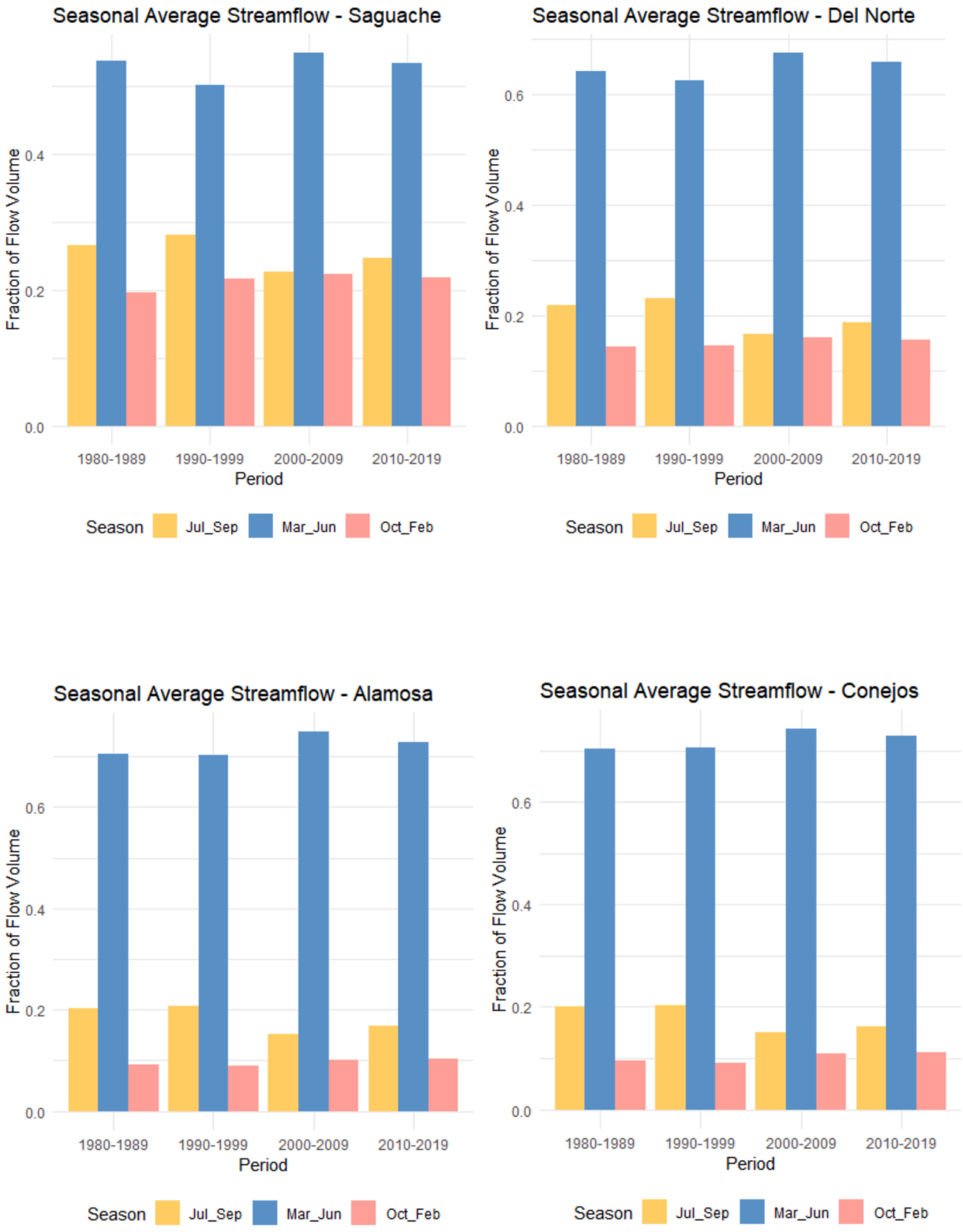

Fig. C1. Seasonal average of streamflow volume by watersheds.

The fractional distribution of seasonal average streamflow (Appendix C) highlights a significant finding: the highest flow generation consistently occurs in March-June, contributing significantly more than other seasons. High-flow seasons often coincide with increased hydrological activity, where certain variables like precipitation intensity, snowmelt rates, and soil moisture levels might play a more significant role in explaining streamflow dynamics. Models trained on more diverse data may better capture relationships between these critical variables and streamflow. In contrast, other seasons may experience relatively low-flow conditions, where the influences of variables are less significant yet more difficult to detect due to nonlinear and lag effects. This pattern demonstrates the profound impact of seasonal variations on

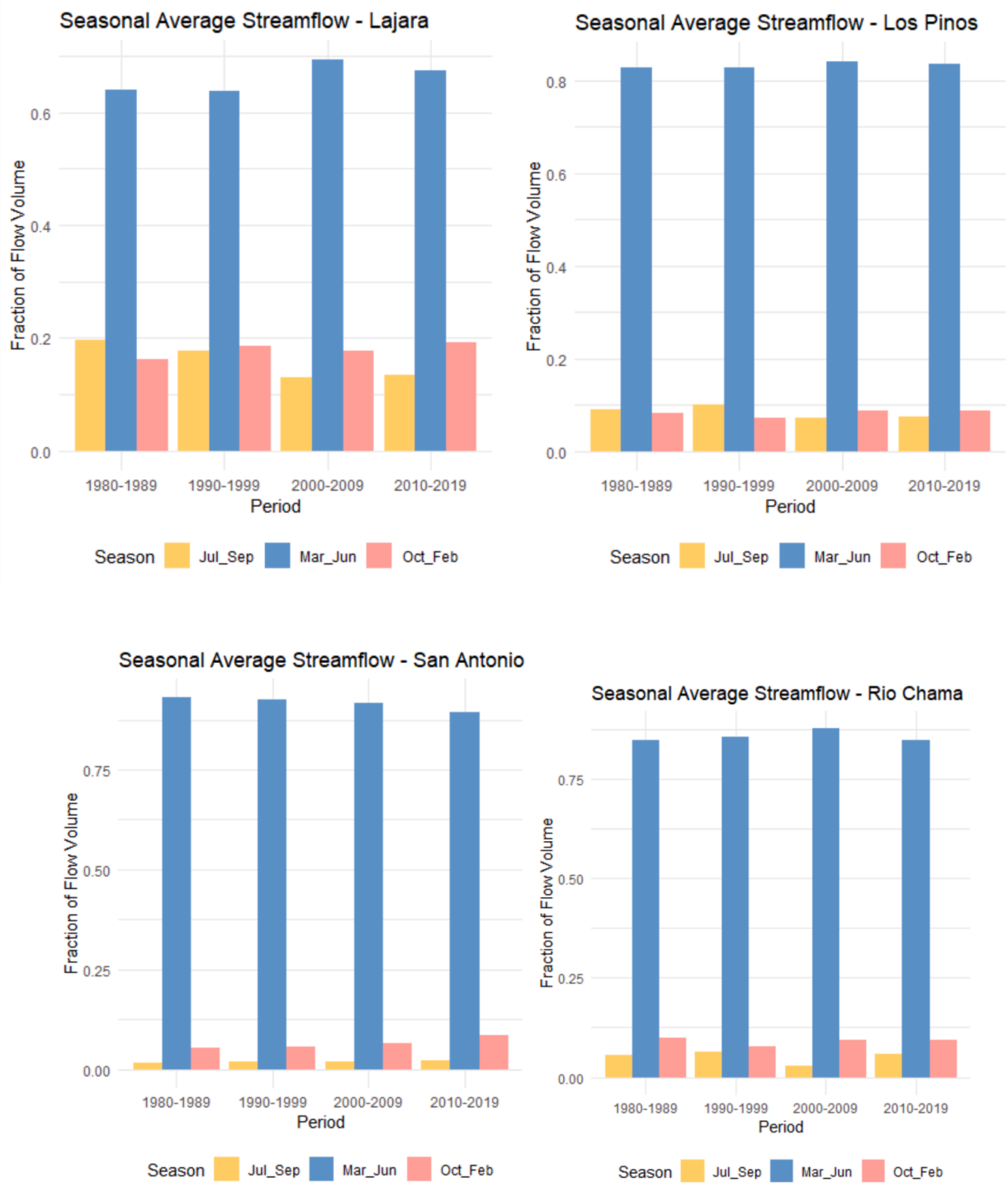

Fig. C1. (*continued*).

streamflow dynamics, a factor researchers should consider in their model development for better predictive accuracy.

Additionally, the changing climate patterns have significantly impacted seasonal stability. Higher elevated watersheds (e.g., Saguache, Del Norte, Alamosa) typically generated a higher percentage of flow from July to September than from October to February (Appendix C). Lower-elevated watersheds (such as Rio Chama, Los Pinos, and San Antonio) showed the opposite pattern. Interestingly, the behavior of the Lajara watershed, situated marginally between lower-higher elevated watersheds, has shifted over time. The initial 20 years (base periods) of the data for the Lajara resembled higher elevated watersheds, but the recent periods showed a different trend, with a higher percentage of streamflow in October-February than July-September—This insight complicates seasonal predictability using stationary regression models and highlights the need to capture evolving hydrologic patterns under climate change. Therefore long-term hydroclimate data (1980 – 2014) was used to develop monthly time-series models for streamflow prediction, validated using data from 2015 to 2019.

The RFR model performed well in accuracy (Table 4), proving ML's capacity to capture nonlinear patterns. The consistency between cross-validation and validation measures (Performance metrics, Supplementary Table) confirmed the models' ability to generalize to new data,

validating the effectiveness of the regularization technique applied to the RFR models.

3.2. Decadal transitions in variable significance

The study also evaluated how the variables influencing streamflow changed over time, comparing historical data from early (1980 – 1999) to recent periods (2000 – 2019). Examining Figs. 11 to 12 reveals a transition in variable influence. Snow cover usually impacts streamflow by gradually releasing meltwater, particularly under warming temperatures and rainfall on snow. However, for Saguache, which is highest in average elevation, the prolonged cooler temperatures might slow down the snowmelt process, resulting in reduced runoff despite snow cover. Figs. 11 and 12 display the watersheds from northern to southern latitudes, with the top rows representing higher-elevation watersheds and the bottom rows showing lower-elevation watersheds.

Notably, snow parameters in Alamosa, Conejos, Del Norte, and Saguache watersheds, characterized by higher elevated and more northern location, showed diminishing effects in recent years, with Conejos exhibiting no impact of snow cover (Fig. 13). Snow albedo followed a similar trend, and soil moisture impact increased across all watersheds in the recent period. Snow depth impacted Rio Chama and San Antonio-Ortiz watersheds during baseline periods, but no significant effect was seen recently.

4. Discussion

Minimum temperature considerably impacts streamflow dynamics through snow accumulation and ablation in higher-elevation watersheds. Snow albedo, snow cover, and snow depth have all played important roles in streamflow dynamics in these basins, although their significance has diminished in recent years. These previously significant factors now exhibit declining predictive influence, which indicates changing hydrological patterns in the region. While these factors had minimal impact during the base periods in specific watersheds (Conejos and Lajara – transitional from higher to lower elevations), they have since decreased, implying that the reducing impact is extending from lower-elevation to higher-elevation watersheds.

The observed reduction of snow effect on streamflow and the concurrent heightened importance of soil moisture indicates the snowpack's evolving dynamics in flow generation, introducing a critical dimension to the discussion. The declining snowpack implies a potential shift in the distribution pathways to the streamflow, raising the possibility that the role of snow in direct streamflow generation may decrease, particularly in downstream areas progressing towards upstream or higher-elevation watersheds. The decreasing contribution of snow to streamflow aligns with the findings across the American West (Li et al., 2017).

A broader view of mechanisms linking snowpack distributions to streamflow may be needed, such as delayed contributions through soil moisture. The results of this analysis provide some clues to these mechanisms. For instance, the reduced snow albedo scores (e.g., Del Norte, Alamosa, and Conejos), as indicated by standardized estimates from 2000 to 2019, suggest more heat absorption, which is further corroborated by rising average minimum temperature, potentially leading to snow melting or augmenting soil moisture.

Notably, frozen soil moisture routed from snowpack may play a prominent role as an acting reservoir, contributing to the streamflow as a delayed effect once thawed. When looking at the significant model intercept with few or no essential predictors, the assumed carryover effect supports the idea of a delayed impact. This lag effect is particularly noticeable in the late summer and fall transition (Fig. 7), which aligns with the hypothesis that frozen soil moisture melts in the summer season, contributing gradually to late summer flow. The melting moisture could also contribute through subsurface pathways, further delaying its effect on streamflow. Additionally, the overall snowpack reduction diminishes the snow factors' influences on streamflow, allowing other factors—particularly soil moisture—to become more influential. The quantity and timing of these changes should geographically vary throughout the year, which poses challenges to capture in simulations.

This study's subdivision of water year enabled analyzing seasonal variability in variable influences. Spanos (2010) argues that traditional model selection criteria (e.g., AIC, BIC) often neglect model validation and error probabilities, leading to unreliable inferences; it indicates the need to address model uncertainty through validation steps. The study's BIC-BMA-based model captures both indirect (lag) and combined effects while quantifying the direct contributions of predictors and is validated against independent streamflow data. The performance of BIC-BMA models at seasonal time scales highlights the significance of incorporating Bayesian approaches for enhanced predictive accuracy. Sometimes, even without individually significant predictors, their combination yields favorable validation results. While the BIC-BMA-based approach has strength in capturing linear patterns within seasonal scales, critically assessing its potential limitations for longer temporal scales is essential because the linear relationship between predictors and the target variables may not always capture the complex hydrologic systems.

Aligning with past results, RFR excels in simulating long-term streamflow, demonstrating its ability to explain intricate hydrologic relationships over an extended duration. Gini impurity revealed varying combined effects of different variables rather than distinct significant predictors in the summer flow season, which indicates nonlinear relationship patterns of the variable influences in some months. However, RF is less interpretable than linear models; although it provides predictors' relative importance, it can be challenging to understand the specific contributions of individual predictors. Conversely, BIC-BMA-based standardized estimates identified important variables and quantified variables' seasonal impact. Applying both methods unveiled various aspects of hydrologic responses, raising questions about computational efficiency and applicability of singular approaches in diverse hydrological contexts. Thus, the implication extends the need to refine conventional approaches and explore integrated methods to improve hydrological modeling performance.

The study has detected the presence of additional factors, such as a carryover or storage impact, but their contributions to streamflow were not explicitly quantified. Further studies should address these limitations and incorporate factors such as groundwater input and storage dynamics. Future research might focus on quantifying the lag effect to capture the system's complexity and delineate historical changes in subseasonal scales. We recommend that future studies explore region-specific high-resolution snow monitoring datasets to estimate snow fraction and refine the results.

The results of the study inform hydrologic modeling in snow-dominated systems. Knowing more about the relative importance of meteorology (air temperature, precipitation) and how water is partitioned on the landscape scale (i.e., soil moisture vs snowpack) helps define what to measure and where to improve understanding of the mechanisms driving streamflow. This also applies to hydrologic modeling – process-based models will not provide robust predictions if their representation of these partitioning mechanisms is wrong or not spatially resolved enough.

5. Conclusion

The study analyzed the seasonal variability of hydroclimatic factors and long-term trends in streamflow using a 40-year dataset (1980–2019) of monthly time series. Employing multi-model inference, which combines Bayesian model selection with a model averaging approach, the study determined the impacts of predictor variables and addressed uncertainty. While the BIC-BMA regression assumes linear relationships, the RFML model was applied to capture nonlinear patterns at the same temporal scale. BIC-BMA performed effectively alongside RFR in

seasonal predictions, providing proportionality and interpretability, whereas RFR excelled in long-term simulations by capturing complex nonlinear interactions and addressing gaps in linear assumptions. This study's data-driven framework for multi-model inference develops a more comprehensive understanding of mechanisms driving climate-related hydrological shifts.

Results revealed that the streamflow drivers exhibited temporal and spatial variability governed by specific mechanisms. Significant carry-over/lag impacts and synergistic and individualistic effects were identified in the seasonal analyses. The results suggest that snow parameters' impact in predicting streamflow has been reduced, more pronounced in lower-elevation watersheds heading upstream. This change is caused by snowmelt runoff's distributional patterns, which introduce complexities in timing and extent—a potential challenge for traditional modeling approaches. The study's adaptable methodology and focus on critical factors make it valuable for stakeholders, aiding in planning, decision-making, and developing resilient strategies for sustainable water resource management.

CRediT authorship contribution statement

Khandaker Iftekharul Islam: Writing – original draft, Software, Methodology, Investigation, Formal analysis, Conceptualization. **James Matthew Gilbert:** Writing – review & editing, Validation, Resources.

Declaration of competing interest

The authors declare that they have no known competing financial interests or personal relationships that could have appeared to influence the work reported in this paper.

Acknowledgments

The authors appreciate the support provided by the Fisheries Collaborative Program (FCP), the University of California-Santa Cruz, and the National Oceanic and Atmospheric Administration (NOAA). The authors especially thank Miles Daniels for his time spent on technical review and Eric Danner for his administrative review. Also, the USDA Southwest Climate Hub's initial data collection support deserves appreciation.

Appendix A. . BIC-BMA regression scatterplots for seasonal prediction

Appendix B. . Distribution of annual average streamflow volume

Appendix C. . Distribution of seasonal volume of streamflow

Appendix D. Supplementary data

Supplementary data to this article can be found online at https://doi.org/10.1016/j.jhydrol.2025.132684.

Data availability

Data will be made available on request.

References

Acquah, H., 2010. Comparison of Akaike information criterion (AIC) and Bayesian information criterion (BIC) in selection of an asymmetric price relationship. J. Dev. Agric. Econ. https://doi.org/10.5897/JDAE.9000032.

Allaire, J., 2012. RStudio: integrated development environment for R [WWW Document]. URL http://www.rstudio.com/.

Amini, A., Ali, T.M., Ghazali, A.H.B., Aziz, A.A., Akib, S.M., 2011. Impacts of Land-Use Change on Streamflows in the Damansara Watershed, Malaysia. Arab. J. Sci. Eng. 36, 713–720. https://doi.org/10.1007/s13369-011-0075-3.

Amini, S.M., Parmeter, C.F., 2011. Bayesian model averaging in R. J. Econ. Soc. Meas. 36, 253–287. https://doi.org/10.3233/JEM-2011-0350.

Archer, K.J., Kimes, R.V., 2008. Empirical characterization of random forest variable importance measures. Comput. Stat. Data Anal. 52, 2249–2260. https://doi.org/10.1016/j.csda.2007.08.015.

Breiman, L., 2001. Random Forests. Mach. Learn. 45, 5–32. https://doi.org/10.1023/A:1010933404324.

Chapter 7: Rio Grande Basin (Technical Report), 2016. . Bureau of Reclamation, https://www.usbr.gov/climate/secure/docs/2016secure/2016SECUREReport-chapter7.pdf.

Chavarria, S.B., Gutzler, D.S., 2018. Observed Changes in Climate and Streamflow in the Upper Rio Grande Basin. JAWRA J. Am. Water Resour. Assoc. 54, 644–659. https://doi.org/10.1111/1752-1688.12640.

Cho, E., Jacobs, J.M., Jia, X., Kraatz, S., 2019. Identifying subsurface drainage using satellite Big Data and machine learning via Google Earth Engine. Water Resour. Res. 55, 8028–8045. https://doi.org/10.1029/2019WR024892.

Daly, C., Bryant, K., 2013. The PRISM climate and weather system—an introduction. Corvallis PRISM Clim. Group 2.

Daly, C., Taylor, G.H., Gibson, W.P., 1997. The PRISM approach to mapping precipitation and temperature, in: Proc., 10th AMS Conf. on Applied Climatology. pp. 20–23. https://prism.oregonstate.edu/documents/pubs/1997appclim_PRISMapproach_daly.pdf.

Darbandsari, P., Coulibaly, P., 2020. Introducing entropy-based Bayesian model averaging for streamflow forecast. J. Hydrol. 591, 125577. https://doi.org/10.1016/j.jhydrol.2020.125577.

Devia, G.K., Ganasri, B.P., Dwarakish, G.S., 2015. A Review on Hydrological Models. Aquat. Procedia, International Conference on Water Resources, Coastal AND OCEAN ENGINEERING (ICWRCOE'15) 4, 1001–1007. https://doi.org/10.1016/j.aqpro.2015.02.126.

Dewi, C., Chen, R.-C., 2019. Random Forest and Support Vector Machine on Features Selection for Regression Analysis. https://doi.org/10.24507/ijicic.15.06.2027.

Elias, E., James, D., Heimel, S., Steele, C., Steltzer, H., Dott, C., 2021. Implications of observed changes in high mountain snow water storage, snowmelt timing and melt window. J. Hydrol. Reg. Stud. 35, 100799. https://doi.org/10.1016/j.ejrh.2021.100799.

Emiliano, P.C., Vivanco, M.J.F., De Menezes, F.S., 2014. Information criteria: How do they behave in different models? Comput. Stat. Data Anal. 69, 141–153. https://doi.org/10.1016/j.csda.2013.07.032.

Fleming, S.W., Vesselinov, V.V., Goodbody, A.G., 2021. Augmenting geophysical interpretation of data-driven operational water supply forecast modeling for a western US river using a hybrid machine learning approach. J. Hydrol. 597, 126327.

Fox, J., Friendly, G.G., Graves, S., Heiberger, R., Monette, G., Nilsson, H., Ripley, B., Weisberg, S., Fox, M.J., Suggests, M., 2007. The car package. https://www.researchgate.net/publication/229024488_The_car_package.

Garen, D., Perkins, T., Abramovich, R., Julander, R., Kaiser, R., Lea, J., McClure, R., Tama, R., 2011. Snow Survey and Water Supply Forecasting (Technical Report No. 622), Water Supply Forecasting. Natural Resources Conservation Service, USDA, United States.

Garen, D.C., 1992. Improved Techniques in Regression-Based Streamflow Volume Forecasting. J. Water Resour. Plan. Manag. 118, 654–670. https://doi.org/10.1061/(ASCE)0733-9496(1992)118:6(654).

Gascoin, S., Grizonnet, M., Bouchet, M., Salgues, G., Hagolle, O., 2019. Theia Snow collection: high-resolution operational snow cover maps from Sentinel-2 and Landsat-8 data. Earth Syst. Sci. Data 11, 493–514. https://doi.org/10.5194/essd-11-493-2019.

Gelman, A., Goodrich, B., Gabry, J., Vehtari, A., 2019. R-squared for Bayesian Regression Models. Am. Stat. 73, 307–309. https://doi.org/10.1080/00031305.2018.1549100.

Gibbons, J.M., Cox, G.M., Wood, A.T.A., Craigon, J., Ramsden, S.J., Tarsitano, D., Crout, N.M.J., 2008. Applying Bayesian Model Averaging to mechanistic models: An example and comparison of methods. Environ. Model. Softw. 23, 973–985. https://doi.org/10.1016/j.envsoft.2007.11.008.

Goldstein, H.L., Reynolds, R.L., Landry, C., Derry, J.E., Kokaly, R.F., Breit, G.N., 2016. The effects of dust on Colorado mountain snow cover albedo and compositional links to dust-source areas, in: AGU Fall Meeting Abstracts. http://adsabs.harvard.edu/abs/2016AGUFM.A21E0106G.

Goodbody, A., 2020. Stream flow data, Natural Resources Conservation Service.

Gregorich, M., Strohmaier, S., Dunkler, D., Heinze, G., 2021. Regression with Highly Correlated Predictors: Variable Omission Is Not the Solution. Int. J. Environ. Res. Public. Health 18, 4259. https://doi.org/10.3390/ijerph18084259.

Grömping, U., 2009. Variable Importance Assessment in Regression: Linear Regression versus Random Forest. Am. Stat. 63, 308–319. https://doi.org/10.1198/tast.2009.08199.

Hastie, T., Friedman, J., Tibshirani, R., 2001. The Elements of Statistical Learning, 2nd ed, Springer Series in Statistics. Springer New York, New York, NY. https://doi.org/10.1007/978-0-387-21606-5.

Hijmans, R.J., Etten, J. van, Sumner, M., Cheng, J., Baston, D., Bevan, A., Bivand, R., Busetto, L., Canty, M., Fasoli, B., Forrest, D., Ghosh, A., Golicher, D., Gray, J.,

Greenberg, J.A., Hiemstra, P., Hingee, K., Ilich, A., Geosciences, I. for M.A., Karney, C., Mattiuzzi, M., Mosher, S., Naimi, B., Nowosad, J., Pebesma, E., Lamigueiro, O.P., Racine, E.B., Rowlingson, B., Shortridge, A., Venables, B., Wueest, R., 2023. raster: Geographic Data Analysis and Modeling. https://cran.r-project.org/web/packages/raster/index.html.

Hoerl, A.E., Kennard, R.W., 1970. Ridge regression: Biased estimation for nonorthogonal problems. Technometrics 12, 55–67. https://doi.org/10.1080/00401706.1970.10488634.

Holmes, R.N., Mayer, A., Gutzler, D.S., Chavira, L.G., 2022. Assessing the Effects of Climate Change on Middle Rio Grande Surface Water Supplies Using a Simple Water Balance Reservoir Model. Earth Interact. 26, 168–179. https://doi.org/10.1175/EI-D-21-0025.1.

Huang, P.-H., 2017. Asymptotics of AIC, BIC, and RMSEA for Model Selection in Structural Equation Modeling. Psychometrika 82, 407–426. https://doi.org/10.1007/s11336-017-9572-y.

Hussainzada, W., Lee, H.S., 2021. Hydrological Modelling for Water Resource Management in a Semi-Arid Mountainous Region Using the Soil and Water Assessment Tool: A Case Study in Northern Afghanistan. Hydrology 8, 16. https://doi.org/10.3390/hydrology8010016.

Islam, K.I., 2023. Predicting areal extent of groundwater contamination through geostatistical methods exploration in a data-limited rural basin. Groundw. Sustain. Dev. 23, 101043. https://doi.org/10.1016/j.gsd.2023.101043.

Islam, K.I., 2021. A Water Informatics Approach to Explore Outcomes of Ground Water and Surface Water Modeling Tools (PhD Thesis). New Mexico State University.

Islam, K.I., 2019. An efficient forecast of hydrologic response for water resources management (Technical Report No. swra-2018-19). New Mexico Water Resources Research Institute.

Islam, K.I., 2015. A Model of Indicators and GIS Maps for the Assessment of Water Resources. J. Water Resour. Prot. 7, 720–726. https://doi.org/10.4236/jwarp.2015.713079.

Islam, K.I., Brown, C.P., 2018. An approach for efficient surface prediction of water-quality parameter, in: AGU Fall Meeting Abstracts. pp. GH33B-1242.

Islam, K.I., Elias, E., Brown, C., James, D., Heimel, S., 2022. A Statistical Approach to Using Remote Sensing Data to Discern Streamflow Variable Influence in the Snow Melt Dominated Upper Rio Grande Basin. Remote Sens. 14, 6076. https://doi.org/10.3390/rs14236076.

Islam, K.I., Elias, E., Brown, C.P., 2019. Water Informatics approach to analyze the dynamics of surface water runoff with climate change. AGU Fall Meeting Abstracts. H33M–H.

Islam, K.I., Elias, E., Carroll, K.C., Brown, C., 2023. Exploring Random Forest Machine Learning and Remote Sensing Data for Streamflow Prediction: An Alternative Approach to a Process-Based Hydrologic Modeling in a Snowmelt-Driven Watershed. Remote Sens. 15, 3999. https://doi.org/10.3390/rs15163999.

Islam, K.I., Gilbert, J.M., 2024. Sensitivity Analysis of Multi-Objective Systems in Alternative Water Resource Operations. Presented at '2024 AGU Fall Meeting. on Dec. Washington D.C., USA'. https://agu.confex.com/agu/agu24/meetingapp.cgi/Paper/1565916.

Islam K.I., Gilbert J.M., 2024. Land Use Dynamics with Water Availability in the Bay-Delta Area and Central Valley, California. Presented at 'Bay-Delta Science Conference' Sacramento, CA., USA' on Sep 30-Oct 2, 2024.

Islam, K.I., Khan, A., Islam, T., 2015. Correlation between atmospheric temperature and soil temperature: a case study for Dhaka. Bangladesh. Atmospheric Clim. Sci. 5, 200. https://doi.org/10.4236/acs.2015.53014.

Jimeno-Sáez, P., Martínez-España, R., Casalí, J., Pérez-Sánchez, J., Senent-Aparicio, J., 2022. A comparison of performance of SWAT and machine learning models for predicting sediment load in a forested Basin. Northern Spain. CATENA 212, 105953. https://doi.org/10.1016/j.catena.2021.105953.

Kim, C., Kim, C.-S., 2021. Comparison of the performance of a hydrologic model and a deep learning technique for rainfall- runoff analysis. Trop. Cyclone Res. Rev. 10, 215–222. https://doi.org/10.1016/j.tcrr.2021.12.001.

Kim, H.-J., Chen, H.-S., Midthune, D., Wheeler, B., Buckman, D.W., Green, D., Byrne, J., Luo, J., Feuer, E.J., 2023. Data-driven choice of a model selection method in joinpoint regression. J. Appl. Stat. 50, 1992–2013. https://doi.org/10.1080/02664763.2022.2063265.

Kim, S., Alizamir, M., Kim, N.W., Kisi, O., 2020. Bayesian Model Averaging: A Unique Model Enhancing Forecasting Accuracy for Daily Streamflow Based on Different Antecedent Time Series. Sustainability 12, 9720. https://doi.org/10.3390/su12229720.

Kostadinov, T.S., Schumer, R., Hausner, M., Bormann, K.J., Gaffney, R., McGwire, K., Painter, T.H., Tyler, S., Harpold, A.A., 2019. Watershed-scale mapping of fractional snow cover under conifer forest canopy using lidar. Remote Sens. Environ. 222, 34–49. https://doi.org/10.1016/j.rse.2018.11.037.

Lapp, S., Byrne, J., Townshend, I., Kienzle, S., 2005. Climate warming impacts on snowpack accumulation in an alpine watershed. Int. J. Climatol. 25, 521–536. https://doi.org/10.1002/joc.1140.

Larsen, L., Gilbert, J.M., Coles, V., Christopher, C., Thakur, G., Islam, K.I., 2024. Collaboratories for Equitable and Resilient Futures I Oral, in: AGU24. AGU. https://agu.confex.com/agu/agu24/meetingapp.cgi/Session/232276.

Lehner, F., Wahl, E.R., Wood, A.W., Blatchford, D.B., Llewellyn, D., 2017. Assessing recent declines in Upper Rio Grande runoff efficiency from a paleoclimate perspective. Geophys. Res. Lett. 44, 4124–4133. https://doi.org/10.1002/2017GL073253.

Leta, O., El-Kadi, A., Dulai, H., Ghazal, K., 2018. Assessment of SWAT Model Performance in Simulating Daily Streamflow under Rainfall Data Scarcity in Pacific Island Watersheds. Water 10, 1533. https://doi.org/10.3390/w10111533.

Li, D., Wrzesien, M.L., Durand, M., Adam, J., Lettenmaier, D.P., 2017. How much runoff originates as snow in the western United States, and how will that change in the future? Geophys. Res. Lett. 44, 6163–6172. https://doi.org/10.1002/2017GL073551.

Li, M., Zhang, Y., Wallace, J., Campbell, E., 2020. Estimating annual runoff in response to forest change: A statistical method based on random forest. J. Hydrol. 589, 125168. https://doi.org/10.1016/j.jhydrol.2020.125168.

Liao, C., Zhuang, Q., 2017. Quantifying the Role of Snowmelt in Stream Discharge in an Alaskan Watershed: An Analysis Using a Spatially Distributed Surface Hydrology Model. J. Geophys. Res. Earth Surf. 122, 2183–2195. https://doi.org/10.1002/2017JF004214.

Liaw, A., Wiener, M., 2002. Classification and regression by randomForest. R News 2, 18–22.

Liu, D., Fan, Z., Fu, Q., Li, M., Faiz, M.A., Ali, S., Li, T., Zhang, L., Khan, M.I., 2020. Random forest regression evaluation model of regional flood disaster resilience based on the whale optimization algorithm. J. Clean. Prod. 250, 119468. https://doi.org/10.1016/j.jclepro.2019.119468.

Liu, Z., Liu, P.-W., Massoud, E., Farr, T.G., Lundgren, P., Famiglietti, J.S., 2019. Monitoring groundwater change in California's central valley using sentinel-1 and grace observations. Geosciences 9, 436. https://doi.org/10.3390/geosciences9100436.

Ma, J., Cheng, J.C.P., 2016. Identifying the influential features on the regional energy use intensity of residential buildings based on Random Forests. Appl. Energy 183, 193–201. https://doi.org/10.1016/j.apenergy.2016.08.096.

Marshall, A.M., Abatzoglou, J.T., Link, T.E., Tennant, C.J., 2019. Projected Changes in Interannual Variability of Peak Snowpack Amount and Timing in the Western United States. Geophys. Res. Lett. 46, 8882–8892. https://doi.org/10.1029/2019GL083770.

Medel, C.A., Salgado, S.C., 2013. Does the bic estimate and forecast better than the AIC? Rev Análisis Económico 28, 47–64. https://doi.org/10.4067/S0718-88702013000100003.

Mocko, D., 2012. NLDAS Mosaic Land Surface Model L4 Monthly 0.125 x 0.125 degree V002 (NLDAS_MOS0125_M). https://doi.org/10.5067/FYHMG8SQX19M.

Moeser, C.D., Chavarria, S.B., Wootten, A.M., 2021. Scientific Investigations Report (Scientific Investigations Report No. 2021–5138), Streamflow Response to Potential Changes in Climate in the Upper Rio Grande Basin. U.S. Geological Survey.

Neath, A.A., Cavanaugh, J.E., 2012. The Bayesian information criterion: background, derivation, and applications. Wires Comput. Stat. 4, 199–203. https://doi.org/10.1002/wics.199.

Painter, T.H., Skiles, S.M., Deems, J.S., Bryant, A.C., Landry, C.C., 2012. Dust radiative forcing in snow of the Upper Colorado River Basin: 1. A 6 year record of energy balance, radiation, and dust concentrations. Water Resour. Res. 48. https://doi.org/10.1029/2012WR011985.

Papacharalampous, G., Tyralis, H., 2022. Time Series Features for Supporting Hydrometeorological Explorations and Predictions in Ungauged Locations Using Large Datasets. Water 14, 1657. https://doi.org/10.3390/w14101657.

Park, S.-E., 2015. Variations of microwave scattering properties by seasonal freeze/thaw transition in the permafrost active layer observed by ALOS PALSAR polarimetric data. Remote Sens. 7, 17135–17148. https://doi.org/10.3390/rs71215874.

Pechlivanidis, I.G., Crochemore, L., Rosberg, J., Bosshard, T., 2020. What Are the Key Drivers Controlling the Quality of Seasonal Streamflow Forecasts? Water Resour. Res. 56, e2019WR026987. https://doi.org/10.1029/2019WR026987.

Penna, D., Tromp-van Meerveld, H.J., Gobbi, A., Borga, M., Dalla Fontana, G., 2011. The influence of soil moisture on threshold runoff generation processes in an alpine headwater catchment. Hydrol. Earth Syst. Sci. 15, 689–702. https://doi.org/10.5194/hess-15-689-2011.

PRISM Climate Group, Oregon State University, 2014. https://prism.oregonstate.edu.

R, Y.P., R, M., 2023. Enhanced streamflow prediction using SWAT's influential parameters: a comparative analysis of PCA-MLR and XGBoost models. Earth Sci. Inform. 16, 4053–4076. https://doi.org/10.1007/s12145-023-01139-9.

RColorBrewer, S., Liaw, M.A., 2018. Package 'randomforest.' https://cran.r-project.org/web/packages/randomForest/index.html.

Robertson, D.E., Wang, Q.J., 2009. Selecting predictors for seasonal streamflow predictions using a Bayesian joint probability (BJP) modelling approach, in: 18th World IMACS. Presented at the MODSIM Congress, Cairns, Australia.

Rosenberg, E.A., Wood, A.W., Steinemann, A.C., 2011. Statistical applications of physically based hydrologic models to seasonal streamflow forecasts. Water Resour. Res. 47, 2010WR010101. https://doi.org/10.1029/2010WR010101.

Rui, H., Mocko, D., 2018. README Document for North American Land Data Assimilation System Phase 2 (NLDAS-2) Products. Goddard Earth Sciences Data and Information Services Center (GES DISC).

Schneider, D., Molotch, N.P., 2016. Real-time estimation of snow water equivalent in the U pper C olorado R iver B asin using MODIS-based SWE Reconstructions and SNO^{TEL} data. Water Resour. Res. 52, 7892–7910. https://doi.org/10.1002/2016WR019067.

Schoppa, L., Disse, M., Bachmair, S., 2020. Evaluating the performance of random forest for large-scale flood discharge simulation. J. Hydrol. 590, 125531. https://doi.org/10.1016/j.jhydrol.2020.125531.

Scornet, E., 2023. Trees, forests, and impurity-based variable importance in regression, in: Annales de l'Institut Henri Poincare (B) Probabilites et Statistiques. Institut Henri Poincaré, pp. 21–52. https://doi.org/10.1214/21-AIHP1240.

Senent-Aparicio, J., Jimeno-Sáez, P., López-Ballesteros, A., Giménez, J.G., Pérez-Sánchez, J., Cecilia, J.M., Srinivasan, R., 2021. Impacts of swat weather generator statistics from high-resolution datasets on monthly streamflow simulation over Peninsular Spain. J. Hydrol. Reg. Stud. 35, 100826. https://doi.org/10.1016/j.ejrh.2021.100826.

Shultz, D., 2020. Snowpack Data Sets Put to the Test [WWW Document]. Eos. https://doi.org/10.1029/2020EO141900 (accessed 4.10.20).
Slater, L., Villarini, G., 2017. Evaluating the Drivers of Seasonal Streamflow in the U.S. Midwest. Water 9, 695. https://doi.org/10.3390/w9090695.
Spanos, A., 2010. Akaike-type criteria and the reliability of inference: Model selection versus statistical model specification. J. Econom., Specification Analysis in Honor of Phoebus. J. Dhrymes 158, 204–220. https://doi.org/10.1016/j.jeconom.2010.01.011.
Steele, C., Dialesandro, J., James, D., Elias, E., Rango, A., Bleiweiss, M., 2017. Evaluating MODIS snow products for modelling snowmelt runoff: Case study of the Rio Grande headwaters. Int. J. Appl. Earth Obs. Geoinformation 63, 234–243. https://doi.org/10.1016/j.jag.2017.08.007.
Strachan, S., Daly, C., 2017. Testing the daily PRISM air temperature model on semiarid mountain slopes. J. Geophys. Res. Atmospheres 122, 5697–5715. https://doi.org/10.1002/2016JD025920.
Svetnik, V., Liaw, A., Tong, C., Culberson, J.C., Sheridan, R.P., Feuston, B.P., 2003. Random Forest: A Classification and Regression Tool for Compound Classification and QSAR Modeling. J. Chem. Inf. Comput. Sci. 43, 1947–1958. https://doi.org/10.1021/ci034160g.
Taia, S., Erraioui, L., Arjdal, Y., Chao, J., El Mansouri, B., Scozzari, A., 2023. The Application of SWAT Model and Remotely Sensed Products to Characterize the Dynamic of Streamflow and Snow in a Mountainous Watershed in the High Atlas. Sensors 23, 1246. https://doi.org/10.3390/s23031246.
Tran, H., Zhang, J., O'Neill, M.M., Ryken, A., Condon, L.E., Maxwell, R.M., 2022. A hydrological simulation dataset of the Upper Colorado River Basin from 1983 to 2019. Sci. Data 9, 16. https://doi.org/10.1038/s41597-022-01123-w.
Trancoso, R., Phinn, S., McVicar, T.R., Larsen, J.R., McAlpine, C.A., 2017. Regional variation in streamflow drivers across a continental climatic gradient. Ecohydrology 10, e1816.
Uwamahoro, S., Liu, T., Nzabarinda, V., Habumugisha, J.M., Habumugisha, T., Harerimana, B., Bao, A., 2021. Modifications to Snow-Melting and Flooding Processes in the Hydrological Model—A Case Study in Issyk-Kul. Kyrgyzstan. Atmosphere 12, 1580. https://doi.org/10.3390/atmos12121580.
Virro, H., Kmoch, A., Vainu, M., Uuemaa, E., 2022. Random forest-based modeling of stream nutrients at national level in a data-scarce region. Sci. Total Environ. 840, 156613. https://doi.org/10.1016/j.scitotenv.2022.156613.
Weakliem, D.L., 1999. A Critique of the Bayesian Information Criterion for Model Selection. Sociol. Methods Res. 27, 359–397. https://doi.org/10.1177/0049124199027003002.
Xia, Y., Mitchell, K., Ek, M., Sheffield, J., Cosgrove, B., Wood, E., Luo, L., Alonge, C., Wei, H., Meng, J., 2012. NLDAS VIC Land Surface Model L4 Monthly 0.125\times 0.125 degree, version 002, Goddard Earth Sciences Data and Information Services Center (GES DISC). https://doi.org/10.5067/ZO0X4QAX5WTD.
Xu, F., Jia, Y., Niu, C., Liu, J., Hao, C., 2018. Changes in Annual, Seasonal and Monthly Climate and Its Impacts on Runoff in the Hutuo River Basin. China. Water 10, 278. https://doi.org/10.3390/w10030278.
Zhang, X., Srinivasan, R., Bosch, D., 2009. Calibration and uncertainty analysis of the SWAT model using Genetic Algorithms and Bayesian Model Averaging. J. Hydrol. 374, 307–317. https://doi.org/10.1016/j.jhydrol.2009.06.023.
Zhang, Y., Touzi, R., Feng, W., Hong, G., Lantz, T.C., Kokelj, S.V., 2021. Landscape-scale variations in near-surface soil temperature and active-layer thickness: Implications for high-resolution permafrost mapping. Permafr. Periglac. Process. 32, 627–640. https://doi.org/10.1002/ppp.2104.
Zhao, H., Li, H., Xuan, Y., Li, C., Ni, H., 2022. Improvement of the SWAT Model for Snowmelt Runoff Simulation in Seasonal Snowmelt Area Using Remote Sensing Data. Remote Sens. 14, 5823. https://doi.org/10.3390/rs14225823.